PHILOSOPHICAL TRANSACTIONS OF THE ROYAL SOCIETY A MATHEMATICAL, PHYSICAL & ENGINEERING SCIENCES

A New Estimate of the Mass of Molecular Gas in the Galaxy and its Implications

C. L. Bhat, C. J. Mayer and A. W. Wolfendale

Phil. Trans. R. Soc. Lond. A 1986 **319**, 249-289
doi: 10.1098/rsta.1986.0099

Phil. Trans. R. Soc. Lond. A **319**, 249–289 (1986) [249]
Printed in Great Britain

A NEW ESTIMATE OF THE MASS OF MOLECULAR GAS IN THE GALAXY AND ITS IMPLICATIONS

BY C. L. BHAT†, C. J. MAYER AND A. W. WOLFENDALE, F.R.S.
Department of Physics, The University, Science Laboratories, South Road, Durham, DH1 3LE, U.K.

(*Received* 4 *November* 1985)

CONTENTS

† On leave from Bhabha Atomic Research Centre, Nuclear Research Laboratory, Srinagar, Kashmir, India.

The amount of gas in the Galaxy and its distribution, both in space and between its various components, are among the 'constants' of the Galaxy. Clearly, this knowledge is a prerequisite for models of star formation, the chemical evolution of the interstellar medium and the manner of evolution of the Galaxy as a whole.

The 21 cm hydrogen-line observations have led to a rather precise derivation of the distribution of atomic hydrogen (HI), but the way in which the important, clumpy, molecular hydrogen (H_2) is distributed has been the subject of much discussion; it is this component that is the principal concern of the present work.

We have examined a variety of data, including that from cosmic γ-rays, X-rays, infrared and millimetre-wave astronomy to compute the manner in which the surface density of H_2 varies with Galactocentric distance. The conclusion is that, in the inner Galaxy, the surface density is much less than previously thought. The total mass of H_2 in the inner Galaxy is estimated to be *ca.* $6.1 \times 10^8\ M_\odot$, a value only some 60% of that in atomic hydrogen.

1. Introduction

The amount of gas in the Galaxy and its distribution, both in space and between its various components, constitute some of the most important parameters of the Galaxy. For example, a knowledge of these parameters is a prerequisite for theories dealing with star formation and the chemical evolution of the interstellar medium, as also with the manner of evolution of the Galaxy as a whole.

Observations of the 21 cm line of atomic hydrogen (HI) have led to a relatively precise derivation of the distribution and amount of this component in the interstellar medium (ISM). However, it is only in recent years that it has been possible to determine the amount of molecular hydrogen (H_2). Early observations (Scoville & Solomon 1975) indicated that H_2 was the dominant component in the inner Galaxy, and although more extensive observations carried out subsequently (Sanders, Solomon & Scoville (1984), hereafter S.S.S.) have reduced the amount of H_2 somewhat, this result still appeared to hold.

In a recent paper (Bhat *et al.* (1985), hereafter referred to as paper I), we argued that even this reduced mass of H_2, specifically $3.2 \times 10^9\ M_\odot$ for Galactocentric distances $R < 10$ kpc (S.S.S.), was an overestimate and that the true value in the inner Galaxy is *ca.* $6.5 \times 10^8\ M_\odot$, a value to be compared with *ca.* $10^9\ M_\odot$ for HI. (In the present work the distance to the Galactic Centre is taken as 10 kpc. We are mindful that the I.A.U. has very recently recommended 8.5 kpc instead (I.A.U. Delhi, 1985). However, most of the arguments in the paper concern relative quantities (e.g. H_2/HI) and these are not affected.) The revised value was based on

γ-ray estimates of the total gas content of the Galaxy (H I plus H_2) with supporting evidence from measurements carried out in several other wavelength regions.

The reasons for the uncertainty in the mass of H_2 in the Galaxy are well known. The H_2 molecule is itself undetectable under the conditions of high density and low temperature that characterize the bulk of the molecular gas present in the Galaxy. Thus the measurements have to be indirect, involving use of a more easily detectable but less abundant trace molecule. Most global surveys have employed the $J = 1 \rightarrow 0$ transition of ^{12}CO (see, for example, Dame 1984; S.S.S.), although extensive observations are now becoming available in the $J = 1 \rightarrow 0$ line of ^{13}CO (Liszt *et al.* 1984). The problem is then an obvious one: how to transform the observed quantity $\int T^{12}\mathrm{d}v$, the velocity-integrated ^{12}CO line temperature along a given line of sight, to a column density of H_2, $N(H_2)$ molecules cm^{-2}? As in paper I, we shall denote the conversion factor between these two quantities by α_{20}, where $2N(H_2) = \alpha_{20} \int T^{12}\mathrm{d}v$ and α_{20} has units of 10^{20} atoms cm^{-2} K^{-1} km^{-1} s. (Other authors prefer to use X rather than α, where $X = N(H_2)/\int T^{12}\mathrm{d}v$. Thus, $X = \alpha_{20}/2$ and has units of 10^{20} molecules cm^{-2} K^{-1} km^{-1} s). Much of the discrepancy between the mass estimates of different groups can be traced to the different methods that are used to determine α_{20}, although there is, in fact, still considerable disagreement about the quantity and distribution of the ^{12}CO. Returning to α_{20} itself, there has come the realization (see, for example, Williams 1985) that it is a function of a variety of physical properties of the region in question. Thus calibration over long path lengths is subject to problems, as is the use of calibration from one region to apply to another. In what follows we assume that α_{20} is simply a function of Galactocentric distance, R, since some, at least, of the properties seem to vary rather smoothly with R. It is realized that this is still an oversimplification although it is an improvement on most previous work, which has assumed that α_{20} is constant everywhere.

In paper I we took as our starting point the ^{12}CO radial distribution of S.S.S. Then, based on γ-ray observations of some nearby molecular clouds, we derived a local value of 2.7 for α_{20}. This value can be compared with 7.2 adopted by S.S.S. and values in the range 4–6 used by other workers. Moving to smaller values of R, the γ-ray emissivity of the molecular ring at $R \approx 6$ kpc showed that even this smaller local value cannot apply throughout the inner Galaxy and a further significant reduction in α_{20} seemed necessary. Interestingly, related analyses based on measurements carried out at other wavelengths also pointed in the same direction. Thus, it was found that $\alpha_{20} \approx 1.4$ at $R \approx 6$ kpc and we tentatively attributed this smaller value to the effects of a 'metallicity' correction (following Blitz & Shu 1980). This correction comes about because it is argued that the higher abundances of metals relative to hydrogen, as observed in the inner Galaxy (see, for example, Pagel & Edmunds 1981), may lead to a correspondingly larger value of the CO/H_2 ratio in that region (see paper I for further details and references). By way of contrast, in a comprehensive analysis of their high-resolution ^{12}CO observations, S.S.S. have argued that $\alpha_{20} = 7.2$, as derived by them locally, should be applicable throughout the Galactic disc.

In this paper we examine in more detail the local calibration methods and conclude that all of them are consistent with $\alpha_{20} = 2$–4. With regard to the inner Galaxy, we disagree with the method adopted by S.S.S. to justify a continuation of $\alpha_{20} = 7.2$ there (and, indeed, the other workers who have adopted R-independent values of α_{20}). We argue that one cannot *a priori* assume that the local calibrations apply in the inner Galaxy, since the methods that led to the calibrations are not available there; we thus discuss other evidence, specifically from infrared,

PHILOSOPHICAL TRANSACTIONS OF THE ROYAL SOCIETY A MATHEMATICAL, PHYSICAL & ENGINEERING SCIENCES

X-rays and the virial theorem and find that α_{20} may indeed decrease at smaller R. However, the reasons for this reduction now seem to be more subtle, involving excitation and temperature effects as well as metallicity. This new realization follows from the difficulties we have recently encountered in understanding the ^{12}CO and ^{13}CO observations of external galaxies, which, although clearly indicating that there can be large-scale variations in α_{20}, show that metallicity is probably not the only factor affecting it.

The layout of the paper is as follows. In §2 we discuss the CO observations themselves since there are at present major differences between the distributions of CO emissivity computed by various groups. Section 3 describes in detail the various methods we have used to determine α_{20} throughout the Galaxy, i.e. via γ-rays, visual extinction, X-rays, the virial theorem, galaxy counts and infrared. In §4 we derive limits on the H_2 content of the Galaxy and the Galactic centre based on the α_{20} values derived in §3 and the CO distributions of §2. Some consequences of these distributions are discussed in §5, and §6 extends the discussion to external systems.

2. The radial distribution of the ^{12}CO emissivity

The radial distribution of the ^{12}CO emissivity is obtained from the observations of the antenna temperature $T_A^*(l, b, v)$, by an unfolding procedure based on an adopted rotation curve for the Galaxy and a model for the z (i.e. vertical) distribution of ^{12}CO (for details see S.S.S.). There have been two recent surveys that sample sufficient data away from $b = 0°$ to derive the scale height of the ^{12}CO gas in the Galaxy: by S.S.S. and the Columbia survey reported by Dame (1984). Both surveys adopt a z distribution for the emissivity function $J(z, R)$ given by

$$J(z, R) = J_0(R) \exp -[\{z - z_c(R)\}/1.2z_{\frac{1}{2}}(R)]^2, \quad (1)$$

where J_0 is the mid-plane emissivity in units of K km s^{-1} kpc^{-1}, and so the results of their fittings are directly comparable. The results obtained for $z_c(R)$ and $z_{\frac{1}{2}}(R)$ are quite similar for the two groups. However, although the shape of $J_0(R)$ is the same for both surveys, it is found necessary to scale the Columbia values upwards by a factor of 2.4 to obtain the same absolute values as reported by S.S.S.

Other derivations of J have been restricted to $b = 0°$ and, because there is known to be a pronounced displacement of the maximum ^{12}CO emission away from $b = 0°$ (Cohen & Thaddeus 1977), these are likely to underestimate the total ^{12}CO in the Galaxy and cannot be directly compared with the overall distributions of S.S.S. and Dame. In figure 1, therefore, we show $J(z, R)$ from S.S.S. and Dame, evaluated for $z = 0$ only, along with the ^{12}CO emissivity results of the other groups obtained for $b = 0°$. It is evident from the figure that appreciable differences exist among the various distributions, and it is tempting at first sight to ascribe them to possible disparities in the absolute calibrations of the different surveys. However, on closer examination, this seems not to be the case because calibration uncertainties are believed to lie between 20 and 30% only (T. M. Dame and D. B. Sanders, personal communications; see also comments by Robinson *et al.* (1984)). A second possibility lies in the weightings that are applied to the data during the unfolding. That this can make a substantial difference to the resulting emissivity distribution can be seen by comparing the results of Burton & Gordon (1978) with those of Robinson *et al.* (1984). In spite of different samplings and coverage, the longitudinal distributions of the velocity-integrated line temperature of Burton & Gordon (1978) and Robinson *et al.* (1984) are remarkably similar in both magnitude and shape and yet the unfolded

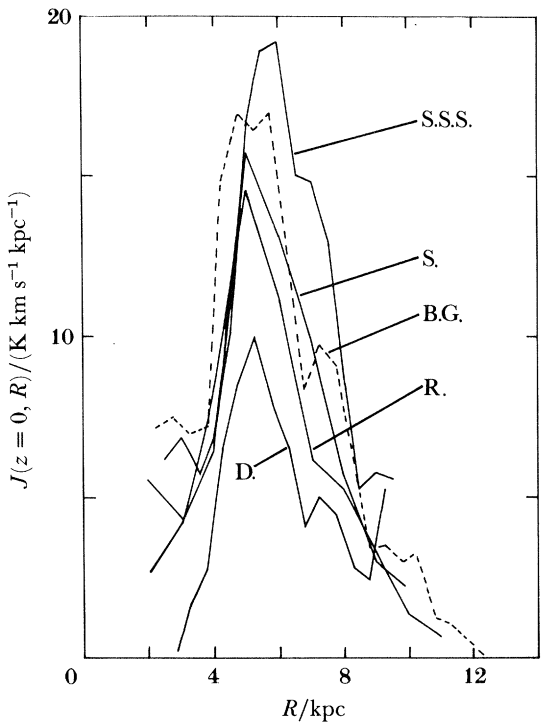

FIGURE 1. The distribution of CO emissivity in the Galactic plane $J(z = 0, R)$ as determined by various authors: S.S.S. (Sanders, Solomon & Scoville 1984), S. (Sanders 1981), B.G. (Burton & Gordon 1978), R. (Robinson *et al.* 1984), D. (Dame 1984). In accordance with the discussion of S.S.S., the values from Burton & Gordon (1978) have been divided by a factor 1.4.

emissivities in the former case are found to lie (figure 1) consistently above those of Robinson *et al.* (1984). It should be mentioned that this comparison was made after the values from Burton & Gordon (1978) had been divided by a factor 1.4, in accordance with the discussion in S.S.S.

In an attempt to understand why this difference comes about, the radial emissivities have been used to predict the velocity-integrated ^{12}CO line temperature, $\int T^{12}\mathrm{d}v$, as a function of l and b (or along $b = 0°$, where only $J(z = 0, R)$ was available) to see how well the emissivities fitted the data. Obviously, such a procedure will give only a smoothed distribution of $\int T^{12}\mathrm{d}v$, which cannot hope to reproduce the true rapidly fluctuating distribution. Nevertheless, we would expect that it should fit in some 'average' sense and at least indicate the underlying trend. Qualitatively, we find that whereas Dame's emissivity distribution consistently underestimates the observed $\int T^{12}\mathrm{d}v$, the emissivities from both S.S.S. and Burton & Gordon overestimate it. In Robinson *et al.* (1984), on the other hand, there appears to be a reassuringly close agreement. It should be noted that we have compared in each case the integrations of the emissivity distribution along the line of sight with the profile of $\int T^{12}\mathrm{d}v$ as a function of l and/or b from which those distributions were derived; absolute calibration uncertainties are therefore not a problem. The results of this comparison for the data of Robinson *et al.* (1984) and S.S.S. are shown in figures 2 and 3 respectively.

To put the above differences on a more quantitative basis we have determined the factor by which the flux, defined as $\int T^{12}\mathrm{d}v\,\mathrm{d}l\,\mathrm{d}b$ and predicted by the axisymmetric models, differs from the corresponding observed value. The results are given in table 1 for the longitude range

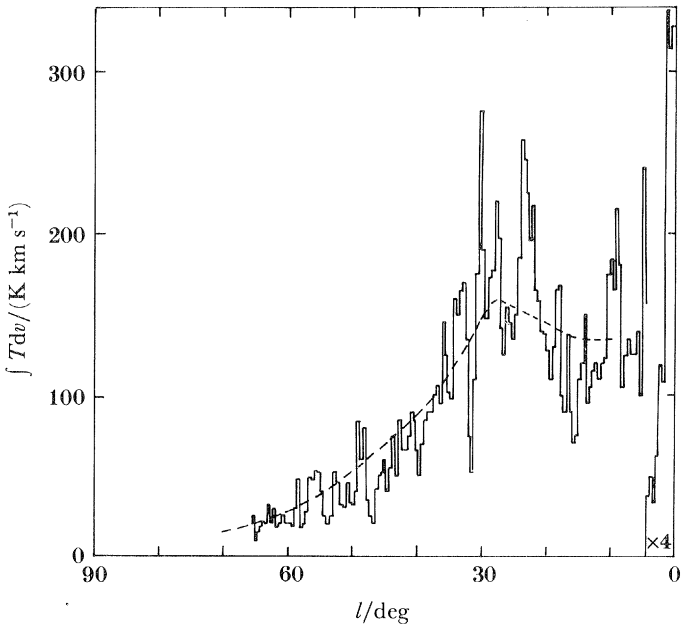

FIGURE 2. Integrated ^{12}CO line temperature as a function of Galactic longitude from the survey of Robinson *et al.* (1984). The broken line is the predicted relation obtained by integrating their unfolded emissivity along the line of sight.

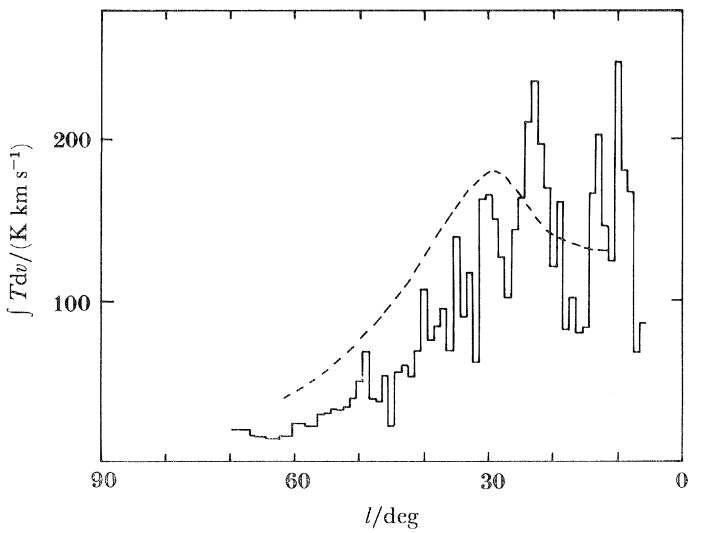

FIGURE 3. Average integrated ^{12}CO line temperature as a function of Galactic longitude from the survey of S.S.S. The integration is for $v \geqslant 0$ km s^{-1} and the average is over seven spectra from $-0.6° \leqslant b^{\mathrm{II}} \leqslant 0.4°$, $\Delta b = 0.2°$, at each l^{II}. The data are taken from Sanders (1981) and the broken line is the predicted relation obtained by integrating the unfolded emissivity along the line of sight.

$l = 12$–$60°$, this being the largest longitude interval common to all the four data sets. The average values listed in table 1 disguise the longitudinal variations that are actually seen between the predictions and the data of different authors. For example, Dame's model fits his data rather well for $l = 40$–$60°$ but underestimates the observed flux for $l = 12$–$40°$. Similarly, S.S.S. achieve a good fit for $l = 12$–$25°$ but overestimate the flux in the remaining range. It

Table 1. Scale factors (as defined in the text) by which emissivity distributions were divided

(The scale factor for S.S.S. was determined from the data in figure 3 taken from Sanders (1981).)

authors	scale factor	region compared	
S.S.S. (1984)	1.3	$12° \leqslant l \leqslant 60°$	$-0.6° \leqslant b \leqslant 0.4°$
Dame (1984)	0.83	$12° \leqslant l \leqslant 60°$	$-1.0° \leqslant b \leqslant 1.0°$
Robinson *et al.* (1984)	1.01	$12° \leqslant l \leqslant 60°$	$b = 0°$
Burton & Gordon (1978)	1.26	$12° \leqslant l \leqslant 60°$	$b = 0°$

is evident from an examination of table 1 that if one uses the ^{12}CO radial distribution of S.S.S., there is the danger of overestimating the amount of ^{12}CO in the Galaxy, while, by adopting Dame's emissivity profile, one would exclude a substantial fraction of ^{12}CO. We have accordingly demanded that the CO line flux (as defined above), predicted by the axisymmetric models, should equal that actually observed The simplest way to achieve this compatibility is to divide the published values of $J_0(z_c)$ by the factors in table 1. This is admittedly rather crude in that no allowance is made for the longitudinal variations that contribute to the mean ratio given in table 1, but in view of the similarity in the overall profile of the two radial emissivity distributions, there seems to be no justification for altering that shape.

The reasons for the differences between the observations and the axisymmetric model predictions are not clear. A possible explanation in the case of S.S.S. is that the corrections that have been applied in going from the emissivity $J(b = 0°)$ to the mid-plane emissivity $J(z_c)$ were too large. S.S.S. state that 'the mid-plane value J_0 is 30%–40% larger than $J(b = 0°)$ because of the warping of the molecular gas layer'. These values come about if one evaluates the exponential in (1) using the values given in their table 2. However, if one compares their figures 5 and 11, which plot their values of mid-plane emissivity and $J(b = 0°)$ for the northern hemisphere, one finds that, in the important region between 5 and 8 kpc, the correction factors lie between 38 and 77%. Other explanations are presumably related to the non-axisymmetric nature of the true CO distribution, different weightings applied to the data at different longitudes and the exact method of unfolding.

Figure 4 shows the final $J(R, z_c)$ adopted in this paper based on the above arguments. The curve corresponding to Robinson *et al.* has been derived by correcting their published $J(R, z = 0)$ by the exponential function given in (1) with the parameters $z_{\frac{1}{2}}(R)$, $z_c(R)$ taken as the mean of the corresponding values from S.S.S. and Dame. The scaling factor between the upper and the lower curves in figure 4 is *ca.* 1.5, still outside the quoted range of uncertainties in the absolute calibrations, whereas that between the middle and lower curves is *ca.* 1.3, which is just about consistent. Part of this discrepancy arises from the different $z_{\frac{1}{2}}(R)$ and $z_c(R)$ derived by the different groups. For example, the scaling factor between the upper and lower curves drops to 1.4 when evaluated at $b = 0°$. Furthermore, of course, the flux values given in table 1 are not absolute and would alter if comparisons were made over different l and b ranges.

To conclude this section, it seems that the additional constraint that the flux predicted by the unfolded axisymmetric CO emissivity distribution should equal the total observed flux from which it is derived, together with differences in absolute calibrations and the distributions of $z_{\frac{1}{2}}(R)$ and $z_c(R)$ removes most, and possibly all, of the discrepancy between the unfoldings of different authors. In the remainder of the paper we shall therefore take the upper and lower curves of figure 4 as upper and lower bounds on the amount of CO present in the Galaxy.

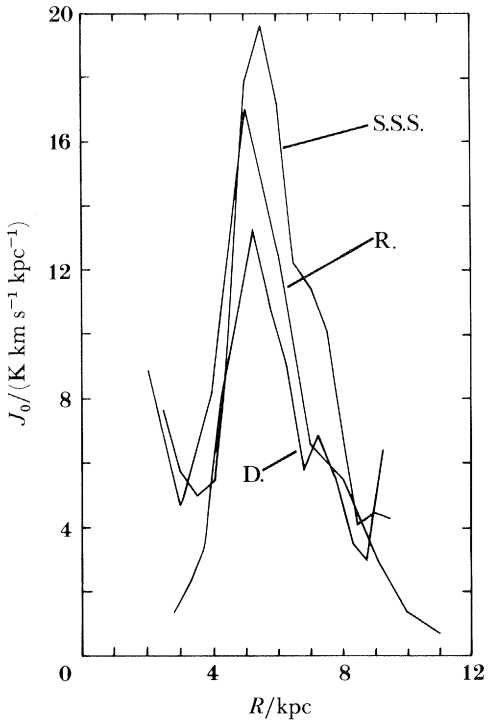

FIGURE 4. Distributions of CO emissivity $J(z_c, R)$ adopted in this paper based on data from S.S.S., Robinson *et al.* (1984), and Dame (1984). The data from Dame (1984) and S.S.S. have been divided by the factors given in table 1. The data from Robinson *et al.* (1984) has been corrected from $z = 0$ to z_c as described in the text.

3. CONVERSION OF $\int T^{12}\mathrm{d}v$ TO COLUMN DENSITY OF MOLECULAR HYDROGEN

3.1. *The γ-ray method*

3.1.1. *Introduction*

To convert the observed ^{12}CO line intensities to the related H_2 column densities, $2N(H_2)$ atoms cm^{-2}, or, equivalently, to convert the radial emissivity profile of the ^{12}CO line to the volume densities of the molecular hydrogen, $n(H_2)$ cm^{-3}, one must determine the parameter α_{20} defined in §1. Several methods have been employed to do this and some of them are mentioned here. Table 2 gives some recent determinations (for a more extensive listing see table 1 of S.S.S.). We discuss here the reasons for the differences between these conversions and argue that, locally, there is essentially no discrepancy between the different methods.

The first method to be considered involves the use of γ-rays.

TABLE 2. VALUES OF THE CO TO H_2 CONVERSION RATIO, α_{20}, USED IN RECENT PUBLICATIONS

authors	α_{20}	method
S.S.S. (1984)	7.2	empirical, local clouds
S.S.S. (1984)	9.2	virial theorem
Lebrun *et al.* (1983)	$\leqslant 6.0$	γ-rays, first galactic quadrant
Bhat *et al.* (1984)	2.7	γ-rays, local clouds
Lebrun & Huang	2.2	empirical, Ophiuchus–Sagittarius region

3.1.2. *Derivation of* α_{20} *locally*

There are several steps in the γ-ray method, the most important being the demonstration that the cosmic rays responsible for the γ-rays (by way of electron bremsstrahlung and pion production by protons) can penetrate the gas clouds and 'see' all the gas. Although there is no doubt that the γ-rays themselves can penetrate the gas, it is conceivable that the cosmic ray particles are kept out of dense regions by the associated magnetic field configurations.

Houston & Wolfendale (1985) have examined the nearby Orion clouds, which are thought to be typical of the Giant Molecular Clouds (GMC) in the Galaxy.

The other important assumption is that the cosmic ray intensity in the vicinity of the local clouds (by local we mean within a few kiloparsecs) is the same as that at the Earth. The evidence for this comes from the observed low anisotropy amplitudes (although admittedly from measurements at higher energies of *ca.* 10^{11} eV) and from the near constancy of cosmic ray intensity over the last 10^9 years.

The value of α_{20} derived by Houston & Wolfendale for the Orion clouds was 3.7 ± 1.0. It should be noted that this value is lower than that of Hermsen & Bloemen (1983), who obtained $\alpha_{20} = 5.2$ owing to the use of a lower local γ-ray emissivity value in that work. Unfortunately a further complication arises with the Orion clouds owing to the possibility that α_{20} is a function of metallicity (defined by the ratio of oxygen to hydrogen; see §1). The Orion clouds are well known to be metal-poor compared with local abundances; specifically, O/H in Orion is one half that in the Sun. If the CO/H_2 ratio decreases as C/H and O/H decrease then the true local value will be $\alpha_{20} \approx 1.8$. There are, however, several factors that would invalidate such an argument. Attempts to interpret the CO observations of external galaxies by a simple metallicity correction are ambiguous (see §6), indicating that parameters other than just metallicity are important in predicting α_{20}. Furthermore, it is not known to what extent the quoted metallicities which are largely determined from spectroscopic observations of H II regions apply to the bulk of the molecular gas when factors other than just the total quantity of C and O determine the gas phase abundances (Williams 1985). In such a situation as many local clouds as possible should be used to derive an average local value of α_{20}. Other local clouds were examined by the γ-ray method by Issa & Wolfendale (1981), and an update of that work (paper I) yielded $\alpha_{20} = 2.3$. Considering all these local values, the likely range of α_{20} locally is 2–4, namely 3 ± 1.

3.1.3. α_{20} *at* $R \approx 6$ kpc

The problem here is related to the possible existence of a large-scale gradient in the cosmic ray distribution. The γ-ray emissivity is the product of gas density and cosmic ray intensity; thus neglecting such a gradient will lead to an overestimate of α_{20}. In paper I we argued in favour of the presence of a cosmic-ray gradient at $R \leqslant 10$ kpc, at least in the electron component, and derived $\alpha_{20} \approx 1.5$ at $R = 6$ kpc.

At this point it is relevant to refer to a similar analysis by Lebrun *et al.* (1983), which resulted in a very wide range for α_{20}: 2–6 for the Galaxy as a whole. Their upper limit was derived by assuming a constant cosmic ray intensity throughout the Galactic disc and for this reason it is expected to give a value larger than those based on local calibrations. The lower limit of Lebrun *et al.* arises when an estimate is made of the extreme magnitude of the discrete source contribution. Although the ensuing value of α_{20} ($= 2.0$) is not far from our preferred value,

we consider it to be based on an overestimate of the discrete source contribution: one of us (A.W.W.) has consistently argued that up to *ca.* 50% of the 2CG catalogue sources (Hermsen 1980) are simply cosmic-ray-irradiated molecular clouds (see, for example, Li *et al.* 1981; Wolfendale 1983), and in a recent paper Houston & Wolfendale (1984) have estimated a total discrete source contribution of *ca.* 20% to the observed γ-ray flux. This leads to $\alpha_{20} \approx 4.8$ from the first Galactic quadrant following the analysis of Lebrun *et al.*, with the upper limit now indicating the neglect of the cosmic ray gradient.

3.1.4. α_{20} *at the Galactic Centre*

The Galactic Centre region is extraordinarily interesting from a number of points of view, not least the possibility that it contains a massive black hole. Claims have been made for the presence of considerable amounts of gas in this region (taken as $R \leqslant 500$ pc), all by way of analyses of the various $\int T^{12}\mathrm{d}v$ measurements. The highest estimate, $M(\mathrm{H_2}) = 3 \times 10^9\ M_\odot$, was by Linke *et al.* (1981); Liszt & Burton (1980) have claimed $1\text{–}2 \times 10^9\ M_\odot$. S.S.S. estimate $3 \times 10^8\ M_\odot$ assuming that their value of $\alpha_{20} = 7.2$ is applicable in this region.

The γ-ray method as applied to the Galactic Centre is not straightforward because of the inevitable uncertainty in the cosmic ray flux. Nevertheless, Bhat *et al.* (1985) have addressed the problem, with the following result: the most reasonable estimate of the cosmic ray intensity is that it is about seven times the local value, a result that comes independently from models involving consideration of the observed intensity of synchrotron radiation, and of the cosmic ray production rate per unit mass of gas being taken to be constant in the Galaxy on the very large scale. The result is that $\alpha_{20} = 0.24$.

As an upper limit to α_{20}, we can consider the situation where the cosmic ray intensity has its lowest reasonable value: the local value. The value of α_{20} then rises by a factor 7, to 1.7.

3.2. *The visual extinction method*

The method labelled 'empirical' in table 2 uses the correlation between $\int T^{12}\mathrm{d}v$ and visual extinction, A_v (defined as referring to 0.55 μm), to obtain α_{20}. The derivation proceeds in several stages and involves correlation of $\int T^{13}\mathrm{d}v$ with star counts (Dickman 1978) or infrared extinction (Frerking *et al.* 1982) to obtain $\int T^{13}\mathrm{d}v/A_\mathrm{v}$ (data from the latter work, for the Taurus cloud, are shown in figure 6). Adopting a uniform gas:dust ratio (Bohlin *et al.* 1978), corresponding to $n(\mathrm{H_2})/A_\mathrm{v} = 0.95 \times 10^{21}$ molecules $\mathrm{cm^{-2}\ mag^{-1}}$ and using the observational constraint that $\int T^{12}\mathrm{d}v / \int T^{13}\mathrm{d}v = 5.5$, gives α_{20}.

Following an analysis of the results of Frerking *et al.* (1982) and Dickman (1978), S.S.S. found that $\int T^{13}\mathrm{d}v$ was approximately proportional to the square root of A_v. As pointed out in paper I, a key question then concerns the effective mean value of $\int T^{13}\mathrm{d}v$ for the GMC that contribute most of the mass of Galactic $\mathrm{H_2}$, since α_{20} now varies from cloud to cloud. S.S.S. have argued from the data of Liszt *et al.* (1981) that this value is 7 K km $\mathrm{s^{-1}}$, leading to $\alpha_{20} = 7.2$, leading to values of α_{20} of 9.8 (see figure 6) and 5.8 for the calibrations of Frerking *et al.* and Dickman respectively. S.S.S.'s preferred value is $\alpha_{20} = 7.2$, close to the mean of these empirical determinations.

Figure 5 shows the data from Liszt *et al.* (1981) plotted as a function of Galactocentric radius R. A near linear gradient is seen to exist in $\int T^{13}\mathrm{d}v$ up to $R \approx 8$ kpc. Assuming that this gradient extends all the way to $R = 10$ kpc, and weighting all the data points equally, we find $\langle \int T^{13}\mathrm{d}v \rangle = 2.1$ K km $\mathrm{s^{-1}}$ locally, whereas, after weighting the data according to the number

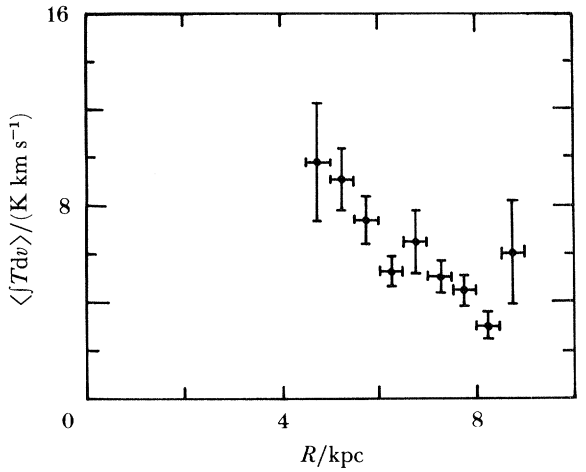

FIGURE 5. Average $\int T\mathrm{d}v$ per cloud as a function of Galactocentric radius from the data of Liszt *et al.* (1981). The error bars are set somewhat arbitrarily to $\langle\int T\mathrm{d}v\rangle/N^{\frac{1}{2}}$, where N is the number of clouds contributing to each radial bin.

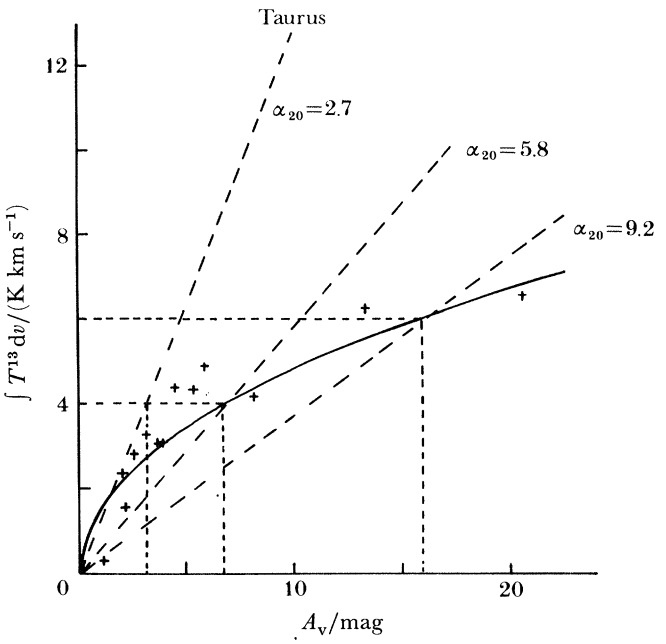

FIGURE 6. The data of Frerking *et al.* (1982) for the Taurus cloud, showing the relation between $\int T^{13}\mathrm{d}v$ and optical extinction. The solid line is the calibration adopted by S.S.S. (1984) and the broken lines show the inferred α_{20}.

of clouds detected in a given radial bin, we obtain $\langle\int T^{13}\mathrm{d}v\rangle = 0.71$ K km s^{-1} at $R = 10$ kpc. It is pertinent to point out that, although a flattening of the gradient for $R > 8$ kpc cannot yet be completely ruled out, it is not supported by the currently available data on nearby molecular clouds. For example, taking the three fully mapped clouds observed by Blitz (1978), the median values of $\int T^{13}\mathrm{d}v$, chosen such that half of the mass of the molecular complex lies within it (see paper I), are 1.7, 1.8 and 1.5 K km s^{-1} for Mon OB2, Mon OB1 and CMa OB1 respectively for an assumed ratio $\int T^{12}\mathrm{d}v/\int T^{13}\mathrm{d}v = 5.5$. Similarly, as shown in paper I, this

ratio leads to a median $\int T^{13}\mathrm{d}v$ of 2 K km s^{-1} for the local cloud complex in Orion. Bearing in mind all these considerations, the unweighted extrapolation of the data of Liszt *et al.* may therefore be used as a representative value of $\langle \int T^{13}\mathrm{d}v \rangle$ per cloud locally, as against 7 K km s^{-1} used by S.S.S. This then leads to $\alpha_{20} = 2.0$ or 2.9, depending upon whether calibration data of Dickman (1978) or Frerking *et al.* (1982) (figure 6) are preferred. The revised values bracket our own calibration based on γ-rays (paper I) and that of Lebrun & Huang (1984), which follows from a 2.6 mm radio survey of the region ($l \approx 10$–$30°$; $b \approx 10$–$20°$). Thus we find there is no discrepancy *locally* between the γ-ray method and the method we have called empirical; both now give values of α_{20} in the range 2–4.

In the inner Galaxy, the data of Liszt *et al.* (1981) show much higher values of $\int T^{13}\mathrm{d}v$ per cloud (figure 5), and a straightforward application of the method of S.S.S. would naturally lead to much larger values for α_{20}. For example, at the peak of the molecular ring ($R \approx 6$ kpc), $\int T^{13}\mathrm{d}v = 9.1$ K km s^{-1}, yielding α_{20} between 7.3 and 14.2 for the respective calibrations of Dickman (1978) and Frerking *et al.* (1982). We argue below that such an approach is invalid because of the origin of the large $\int T^{13}\mathrm{d}v$ for the Taurus region and the GMCs and the physical reasons for the saturation found by Frerking *et al.* (1982).

Figure 6 shows $\int T^{13}\mathrm{d}v$ plotted against A_v for the Taurus dark cloud, together with the fit used by S.S.S. and the linear correlation corresponding to $\alpha_{20} = 2.7$. As mentioned in paper I, a linear relationship can fit the data with $\alpha_{20} \approx 3.8$ up to $A_\mathrm{v} = 6$ magnitudes but, as pointed out by S.S.S., the whole data set is better fitted by $\int T^{13}\mathrm{d}v \propto A_\mathrm{v}^{0.48}$. Frerking *et al.* (1982) have put forward two possible explanations for the turnover in the correlation of $\int T^{13}\mathrm{d}v$ with A_v; namely, (1) it is due to an optical depth saturation effect, and (2) CO is depleted in denser regions by attachment to grains.

If the turnover is due to an optical depth effect then it is important to establish that at a given $\int T^{13}\mathrm{d}v$ the clouds in the inner Galaxy are saturated to the same extent as the Taurus calibration points. This clearly need not be so. If a GMC is made up of a number of sub-clouds offset in velocity from each other, the $\int T^{13}\mathrm{d}v$ from the sub-clouds would add linearly. We shall call this the optically thin case. Without the offsets it would be more appropriate to add the optical depths; this will be called the optically thick case.

In the optically thin case we would expect a broad low-temperature line profile compared with a relatively narrow high-temperature line for the other. Inspection of the data by Frerking *et al.* for the Taurus cloud shows that large $\int T^{13}\mathrm{d}v$ are associated with narrow lines ($\Delta V_\mathrm{FWHM} \approx 1.5$ km s^{-1}) and relatively high temperatures ($T_\mathrm{A}^* \approx 4$ K). In Liszt *et al.* (1981), however, large $\int T^{13}\mathrm{d}v$ in the inner Galaxy are the result of small mean temperatures of 1–1.5 K and large line widths of 6–7 km s^{-1}. One can see immediately that the line shapes themselves strongly support the latter hypothesis, i.e. the large $\int T^{13}\mathrm{d}v$ values encountered in the inner Galaxy are the result of adding together separate cloud regions offset in velocity from each other. It therefore follows that the correct α_{20} to use should come from the slope of the $\int T^{13}\mathrm{d}v$–A_v relation as seen at small A_v.

We turn now to the second possibility put forward by Frerking *et al.* (1982), that the apparent saturation in $\int T^{13}\mathrm{d}v$ at large A_v (figure 6) is caused by CO depletion by accretion onto dust grains in the densest parts of the Taurus clouds. These authors give an effective depletion time of $3 \times 10^9/n(\mathrm{H_2})$ years, $n(\mathrm{H_2})$ being the volume density of the molecular gas, showing that significant depletion can take place on a dynamical timescale for densities greater than 10^4 cm^{-3}. If this were so, then the large values of α_{20} deduced from figure 5 at large $\int T^{13}\mathrm{d}v$ would indeed

be correct for Taurus. Observational evidence for this possibility has been put forward by Whittet *et al.* (1985) based on the detection of an infrared vibrational feature of solid-state CO at 4.67 μm. However, the arguments put forward above about the line shapes need to be considered in this case also, since it is the nonlinearity between $\int T^{13}\mathrm{d}v$ and A_v that does not allow a unique A_v to be deduced from a given observed $\int T^{13}\mathrm{d}v$. Thus, if the large $\int T^{13}\mathrm{d}v$ found by Liszt *et al.* (1981) for the clouds in the inner Galaxy results from an optically thin superposition of subregions within the clouds, as suggested by the observed large velocity dispersions and low temperature, then it is the $\int T^{13}\mathrm{d}v$ of these subregions that should govern the true α_{20} in this case. For illustration, suppose that the mean value $\int T^{13}\mathrm{d}v \approx 7$ K km s^{-1} per cloud, advocated by S.S.S., was the result of a superposition of two identical subregions within the cloud. For compatibility with Liszt *et al.* (1981), the parameters of the subregions would be $T^{13} \approx 1.2$ K, $\Delta V_{\mathrm{FWHM}} \approx 3$ km s^{-1} with a velocity separation of 3 km s^{-1}. The relevant value of α_{20} is then that at $\int T^{13}\mathrm{d}v = 3.5$ K km s^{-1}. Because this value is already on the linear part of the Taurus calibration curve, splitting the cloud into more subregions will not further reduce α_{20}.

It has been shown above that, whatever the reason for the shape of the Taurus calibration curve, it is not valid to use large $\int T^{13}\mathrm{d}v$ for the clouds in the inner Galaxy to justify large values of α_{20}. The large line widths and low aerial temperatures favour the linear part of the calibration curve at low A_v as being the relevant region for the bulk of the GMC. The data of Dickman (1978) and Frerking *et al.* (1982) would then give values of α_{20} of 2.0 and 3.8 respectively for the clouds in the inner Galaxy in spite of their large $\int T^{13}\mathrm{d}v$, provided that these local calibrations are applicable there. In the following sections we shall argue that this assumption is not justified, however, and that the true values are even smaller.

3.3. *X-ray estimates*

3.3.1. *Introduction*

The methods that led to the determination of $\int T\mathrm{d}v/A_\mathrm{v}$ and $N(\mathrm{H}_2)/A_\mathrm{v}$ locally are not available in the inner Galaxy but fortunately there are alternatives. Inevitably the methods described below contain assumptions and uncertainties, as did those described earlier, but in that these are different for different methods, the validity of using these alternative techniques follows from the fact that they lead to mutually consistent results on the values of α_{20}, both locally as well as in the inner Galaxy.

We start with the X-ray technique.

3.3.2. *The principle of the method*

Most of the Galactic X-ray sources (XRS) exhibit a low-energy cut-off in their spectra because soft X-rays suffer absorption in the interstellar medium (ISM) through photoelectric interactions with atoms of low Z, chiefly those of oxygen, carbon, nitrogen and hydrogen (Adams 1980). Detailed calculations made by a number of workers (Brown & Gould 1970; Cruddace *et al.* 1974; Fireman 1974; Ride & Walker 1977; Morrison & McCammon 1983) show that the absorption cross section per atom is not significantly different for the atomic and molecular hydrogen species nor does it sensitively depend upon the ionization state of the absorber atom. Moreover, recent work by Morrison & McCammon (1983) reveals that the effect of grain-blanketing, considered first by Fireman (1974), should in actual practice be sufficiently small to make the interaction cross section essentially independent of whether the absorber

atoms are in the gas or grain phases. Thus, for a given chemical abundance of elements (generally adopted as in Brown & Gould 1970), it should be possible to obtain a reliable estimate of the total gas (HI + H_2 + HII + heavier nuclei) column density present up to an XRS by comparing the observed X-ray spectrum with the production spectrum, i.e. the one that would be seen in the absence of absorption. The latter spectrum, however, is not known *a priori* and, depending upon its assumed form (generally taken as a power-law or thermal bremsstrahlung; see, for example, Jones 1977; Gorenstein *et al.* 1967; Palmieri *et al.* 1971), the X-ray-derived column density, N_X (best fit value, expressed in equivalent hydrogen atoms cm^{-2}) may differ significantly for various model spectra. Moreover, supernova remnants (SNRS) generally exhibit a complicated spectral behaviour and sometimes require consideration of one or more multi-temperature components (Nugent *et al.* 1984), line emission features (Becker *et al.* 1982) and a change in local elemental abundance values (Burginyon *et al.* 1975). A further complication is that some compact XRSS (binary-type) are known to show evidence (Adams 1980; Jones *et al.* 1973) for appreciable circumstellar absorption of soft X-rays, as distinct from the genuine interstellar absorption. Finally, there is also some evidence seen for a time-evolution in the spectra of some XRSS, both on short and long timescales (Branduardi *et al.* 1976). Nevertheless, the method does give independent estimates of gas column density along selected lines of sight.

A consequence of some of the above-mentioned problems is that N_X values quoted by different groups for the same source are occasionally found to differ significantly. However, since the effect of using some spectral fits is to underestimate N_X while that of some others would be to overestimate it, it is likely that the average value $\langle N_X \rangle$, derived from various measurements, should reliably estimate the actual gas column density lying in front of the XRS.

To test the technique we shall compare here $\langle N_X \rangle$ obtained for the Galactic SNRS listed in table 3 with N_v, the corresponding column density predicted by optical extinction (Bohlin *et al.* 1978):

$$N_v = 1.8 \times 10^{21} A_v \text{ (atoms cm}^{-2}\text{)}. \quad (2)$$

Here A_v (magnitudes) is the total visual extinction along the line of sight to the remnant. Equation (2) is based on absorption measurements of the Lyman α line for 100 stars lying at distances of up to 3.4 kpc from the sun and having colour excess $E(B-V)$ values of 0.5 or less. The ratio of the total absorption A_v to selective absorption $E(B-V)$ has been taken as 3.2, following Savage & Mathis (1979), and N_v does not include a correction for the ionized component of the ISM present in HII regions (a correction that could amount to up to *ca.* 10%). It should be noted that SNRS are particularly suitable for the present investigation because they do not exhibit flux variability, which is generally a manifestation of the variable intrinsic absorption observed in several X-ray binary systems. The results are given in figure 7; a good correlation is evident between $\langle N_X \rangle$ and N_v, or, equivalently, between $\langle N_X \rangle$ and A_v, represented by the regression line

$$N_X = (2.05 \pm 0.18) \times 10^{21} A_v^{1.03}. \quad (3)$$

Clearly N_X is very nearly proportional to A_v and in fact over most of the A_v range the fit is close to the result of an earlier analysis made by Gorenstein (1975) and Ryter *et al.* (1975) independently, and both based on a study of only four SNRS:

$$N_X = (2.13 \pm 0.5) \times 10^{21} A_v. \quad (4)$$

PHILOSOPHICAL TRANSACTIONS OF THE ROYAL SOCIETY A MATHEMATICAL, PHYSICAL & ENGINEERING SCIENCES

Table 3. A comparison of N_X with N_v/A_v for various types of Galactic X-ray sources

(Units of 10^{20} atoms cm^{-2}.)

XRS	N_X	N_v	A_v (mag)	source type	references
1. Vela X	0.97 ± 0.57	1.98	0.11	SNR	1–3, 63
2. Cgy Loop	4.0 ± 0.5	5.2 ± 0.5	0.29 ± 0.03	SNR	4–14, 64, 65
3. SN1006	8.8 ± 1.1	13.3 ± 5.2	0.75 ± 0.30	SNR	15–20, 16
4. Pup A	27 ± 2.0	28.0†	1.6†	SNR	2, 3, 4, 21–23, 66
5. Tycho	42.0 ± 2.9	34.0 ± 4.0	1.9 ± 0.2	SNR	18, 24–27, 67, 68
6. Crab	31.0 ± 5.6	26.0 ± 4.0	1.4 ± 0.2	SNR	9, 18, 29–34, 34, 49, 69
7. RCW86	43.3 ± 3.8	33.0 ± 3.0	1.9 ± 0.2	SNR	35, 36, 16, 66
8. Cas A	89.0 ± 8.3	77.0	4.3	SNR	9, 27, 28, 37–44, 34
9. Kepler	80.0 ± 6.3	52.0 ± 13.0	2.9 ± 0.7	SNR	15, 45, 68, 71
10. RCW 103	89.1 ± 3.6	68.0 ± 14.0	3.8 ± 0.8	SNR	35, 45, 46, 70, 71
11. G296.1, −0.7	54.5 ± 5.2	34.0 ± 6.0	1.9 ± 0.3	SNR	47, 72
12. SCO X-1	25.4 ± 1.6	21.0 ± 1.0	1.16 ± 0.04	binary	48–51, 73
13. Cyg X-1	48.4 ± 3.1	61.0 ± 2	3.4 ± 0.13	binary	9, 52, 53, 73–76
14. Cir X-1	200	203	11.2	binary	54, 77
15. Cen X-3	350 ± 70	79.0	4.4	binary	55, 73
16. 4U1728−34	246.0	192.0	10.7	binary	56, 78
17. 4U1735−44	46.0	14.5	0.8	binary	56, 79
18. Grindlay 1	266.0 ± 40	270.0	15.0	glob. cluster	57–59
19. NGC6624	12.0	16.0	0.8	glob. cluster	60, 57
20. NGC1851	35 ± 50	4.0	0.22	glob. cluster	57
21. NGC6441	72	30	1.44	glob. cluster	57, 61, 62
22. NGC7078	10 ± 160	8	0.38	glob. cluster	57
23. NGC6712	10.0	23	1.12	glob. cluster	57
24. Terzan 2	82 ± 50	80	4.4	glob. cluster	57
25. Liller 1	320 ± 50	200	11.1	glob. cluster	57

† A_v quoted by Gorenstein (1975) has been corrected owing to change in the Pup A distance from 2 kpc to 1.2 kpc: $N_X = (1.33\pm0.10)\,N_v-(2.2\pm4.2)$.

References: 1, Kahn *et al.* (1983); 2, Moore & Garmire (1976); 3, Gorenstein *et al.* (1974); 4, Kayat *et al.* (1980); 5, Kahn *et al.* (1980); 6, Rappaport *et al.* (1974); 7, Tuohy *et al.* (1979*a*); 8, Ku *et al.* (1983); 9, Seward *et al.* (1972); 10, Grader *et al.* (1970); 11, Burginyon *et al.* (1975); 12, William *et al.* (1984); 13, Blecker *et al.* (1972); 14, Stevens & Garmire (1973); 15, Becker *et al.* (1980); 16, Zarnecki & Bibbo (1979); 17, Culham (1977); 18, Holt (1983); 19, Smith *et al.* (1985); 20, Davelaer *et al.* (1978); 21, Zarnecki *et al.* (1978); 22, Winkler *et al.* (1981); 23, Seward *et al.* (1971); 24, Pravdo *et al.* (1980); 25, Reid *et al.* (1981); 26, Seward *et al.* (1983); 27, Smith (1981); 28, Charles *et al.* (1979); 29, Charles *et al.* (1973); 30, Fritz *et al.* (1971); 31, Clark *et al.* (1973); 32, Henry *et al.* (1972); 33, Garmier & Riegler (1972); 34, Hill *et al.* (1975); 35, Nugent *et al.* (1984); 36, Winkler (1978); 37, Fabian *et al.* (1980); 38, Murry *et al.* (1979); 39, Pravdo *et al.* (1976); 40, Burginyon *et al.* (1973); 41, Gorenstein *et al.* (1970); 42, Serlemitsos *et al.* (1973); 43, Markert *et al.* (1979); 44, Charles *et al.* (1975); 45, Tuohy *et al.* (1979*b*); 46, Tuohy & Garmire (1980); 47, Markert *et al.* (1981); 48, Pollock *et al.* (1981); 49, Moore *et al.* (1973); 50, Lamb & Sanford (1979); 51, Kahn *et al.* (1984); 52, Page (1981); 53, Bedford *et al.* (1981); 54, Chiapetti & Bell-Burnell (1981); 55, Lien *et al.* (1984); 56, Hertz & Grindlay (1984); 57, Grindlay (1981); 58, Basinka *et al.* (1984); 59, Hoffman *et al.* (1979); 60, Stella *et al.* (1984); 61, Bell-Burnell & Chiappetti (1984); 62, Jones (1977); 63, Ryter *et al.* (1975); 64, Parker (1967); 65, Raymond *et al.* (1981); 66, Gorenstein (1975); 67, Reynolds & Ogden (1978); 68, van den Bergh & Kamper (1977); 69, Miller (1973); 70, Westerlund (1969); 71, Leibowitz & Danziger (1983); 72, Longmore *et al.* (1977); 73, Bradt & McClintock (1983); 74, Margon *et al.* (1973); 75, Bregman *et al.* (1973); 76, Wu *et al.* (1975); 77, Whelan *et al.* (1977); 78, Grindlay & Hertz (1981); 79, Watson *et al.* (1983).

In figure 7 we have also plotted N_X against N_v for several non-SNR type sources listed in table 3. These include binary systems and globular cluster sources, and some of them lie deep in the inner Galaxy. Except for Cen X-3, where the large $\langle N_X\rangle$ is believed to be due to strong X-ray absorption in the stellar wind of the primary (Adam 1980), most of the other sources are found to lie quite close to the line represented by (3). Thus, although it is reassuring to note that in general $\langle N_X\rangle$ gives a reliable estimate of the interstellar gas column density, one should be

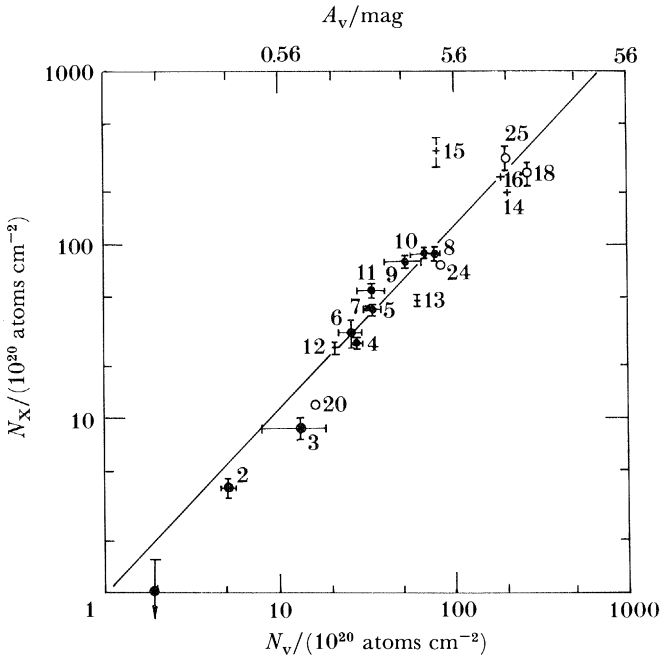

FIGURE 7. The line-of-sight gas column densities $\langle N_X \rangle$, as given by the X-ray absorption technique, are compared with the values $\langle N_v \rangle$ resulting from the optical and infrared extinction studies for three types of Galactic X-ray sources: (●) supernova remnants, (○) globular cluster sources, and (+) the X-ray binary systems, lying at distances of up to 11 kpc from the Sun. Each $\langle N_X \rangle$ represents an average over the values deduced for thermal and power law spectral fits by different workers (these workers generally adopted the elemental abundance values as given by Brown & Gould 1970). Formal $\pm 1\sigma$ error flags are shown in the figure. It is evident that most of the points lie remarkably close to the fitted line, thereby consolidating the previous result by Gorenstein (1975) and Ryter *et al.* (1975) that $\langle N_X \rangle$ is a good measure of the line of sight gas column density. The source Cen X-3 (no. 15) lies significantly away from the line, because of significant additional absorption suffered by X-rays in the immediate source vicinity (this intrinsic absorption explanation follows from the known time variability). We have encountered a few other cases like this among the X-ray binary systems; they represent a constraint on the universal application of the X-ray method.

careful about Cen X-3-like binary systems where circumstellar absorption may lead to a gross overestimation of the true interstellar gas density. Bearing this caution in mind, we shall use $\langle N_X \rangle$ for an XRS, together with the corresponding N(HI) (specifically we use $\langle N_X \rangle = N(\mathrm{HI}) + \alpha_{20} \int T^{12} \mathrm{d}v$) to give α_{20}.

3.3.3. *The local value of* α_{20}

For this purpose we refer to the SNR IC443 (= G 189.1+3.0), which is at a distance of 1.5 kpc (Woltjer 1972) and represents the best known example so far of a likely physical association between an SNR and a molecular gas cloud. This connection is suggested by the fact that the ^{12}CO ridge associated with this cloud corresponds in position and velocity to a 21 cm line absorption feature (Dickel 1973), implying that the molecular cloud, like the HI gas, should be lying in front of the SNR. This inference is further reinforced by the observed anticorrelation of the CO signal with the corresponding optical emission, suggesting visual extinction by dust which is presumably associated with the molecular cloud (Scoville *et al.* 1977).

The cloud is correlated with the central part of the remnant and, for a mean line-width of 3.5 km s^{-1}, corresponding to the spatial extent of the remnant, yields an average

$\int T^{12}\mathrm{d}v = 7.9 \pm 1.2$ K km s^{-1} (Cornett *et al.* 1977; Scoville *et al.* 1977). Image Proportional Counter (IPC) measurements on board the Einstein Observatory (Watson *et al.* 1983; Petre *et al.* 1983) exhibit hardness ratio variations across the remnant that are positionally correlated with the molecular cloud and, for the best-fit SNR temperature range of $(0.6\text{–}1.8) \times 10^7$ K, are consistent with an additional column density of $(30 \pm 10) \times 10^{20}$ atoms cm^{-2} (Petre *et al.* 1983; C. Jones, personal communication). If the latter is assumed to be in the form of H_2, as is suggested by the positional association referred to above, we obtain $\alpha_{20} = (30 \pm 10)/(7.9 \pm 1.2) = 3.8 \pm 1.4$. As an alternative, associating only a part of this extra, X-ray-derived column density with the molecular hydrogen (i.e. treating the rest as N(HI)) will have the obvious effect of lowering α_{20}.

3.3.4. α_{20} *in the inner Galaxy*

Sanders *et al.* (1984) have treated α_{20}, derived by them for local H_2 clouds, as an invariant quantity while estimating $N(H_2)$ as a function of the Galactocentric distance R.

However, we believe that there are many factors that lead to a dependence of α_{20} on R (see Williams 1985). These include the metallicity gradient and temperature gradient and the different fractions of carbon and oxygen in grains and in the gas phase conditioned by temperature and shocks.

The arguments just given are very relevant to the likelihood of α_{20} being a function of R, and it is an important feature of the X-ray technique that the factors that cause the division of material between gas and solid phases do not affect the estimates of the total amount of gas (C, N, O) in the inner Galaxy: the X-rays 'see' all the gas. One correction is necessary, however, and this is to allow for the metallicity itself; that is, the apparent column density of total gas $\langle N_X \rangle$ derived by the X-ray method, with the use of the local calibration (figure 7), must be divided by the appropriate average metallicity along the line of sight.

The XRSS chosen for the present study (table 4) all lie outside the Galactic nucleus (which is treated separately because of its complex nature) along lines of sight for which $\int T^{12}\mathrm{d}v$ values are currently available. They include five SNRS besides nine compact XRSS from the Galactic bulge region ($|b| \leqslant 1°$). For the SNRS, the column density of atomic hydrogen, N(HI), has been obtained by using 21 cm emission and absorption profiles from Radhakrishnan *et al.* (1972) and Caswell *et al.* (1975). The N_X values quoted in the literature are based on the assumption of a constant elemental abundance throughout the Galaxy and are corrected for the presence of the metallicity gradient by dividing $\langle N_X \rangle$ by $\langle M/M_\odot \rangle$, the average metallicity factor from Li *et al.* (1982), suitably weighted for the distribution of gas along the line of sight up to the remnant. For the latter purpose we have used ^{12}CO emissivity radial distribution values from S.S.S. Subtracting N(HI) for the remnant from the metallicity-corrected total gas column density then gives $N(H_2)$, the column density of the molecular gas lying ahead of the SNR. We obtain the corresponding $\int T^{12}\mathrm{d}v$ from S.S.S., making the reasonable assumption that the molecular gas is distributed smoothly along the line of sight to the source and taking only the fraction that should be in front of the remnant. We then divide to derive α_{20}. We designate it α_{20}^+ to emphasize that the X-ray-derived column density, $\langle N_X \rangle$, has been corrected for the expected metallicity effect.

For the non-SNR-type Galactic-bulge XRSS, α_{20}^+ has been derived in essentially the same manner as discussed above. Wherever the source distance is not known independently, it has been taken as 10 kpc from the Sun (an assumption justified in a statistical sense by the

PHILOSOPHICAL TRANSACTIONS OF THE ROYAL SOCIETY A MATHEMATICAL, PHYSICAL & ENGINEERING SCIENCES

PHILOSOPHICAL TRANSACTIONS OF THE ROYAL SOCIETY A MATHEMATICAL, PHYSICAL & ENGINEERING SCIENCES

TABLE 4. α_{20}^{+} ESTIMATES FOR THE INNER GALAXY

XRS	l/deg	b/deg	R/kpc	$\left\langle \frac{M}{M_\odot} \right\rangle$†	$\frac{N_X}{10^{20}\text{ atoms cm}^{-2}}$	$\frac{N(\text{H I})}{10^{20}\text{ atoms cm}^{-2}}$	$\frac{N(\text{H}_2)}{10^{20}\text{ atoms cm}^{-2}}$	$\frac{\int T\,dv}{\text{K km s}^{-1}}$	α_{20}^{+}
W49B (SNR)	43.3	−0.2	7.4	1.64	330±30 (1–3)	102 (17)	99.2±18.3	48	2.1±0.4
W44 (SNR)	34.6	−0.5	7.7	1.32	125±75 (1, 3)	58 (17, 18)	36.7±56.8	30	1.2±1.9
3C391 (SNR)	31.87	−0.02	5.8	1.76	$230^{+520}_{-192.5}$ (4)	67.5 (17)	$631.2^{+295.4}_{-109.4}$	140±60	0.45
G21.5−0.9 (SNR)	21.5	−0.9	5.8	1.63	100 (5)	39.2 (18)	22.2	110±10	0.20
Kes 75 (SNR)	29.7	−0.3	12.4	1.71	500^{+1500}_{-200} (6)	222 (18)	$70.4^{+877.1}_{-117.0}$	150±20	0.47
GX0.2−0.2	+0.204	−0.235	~0.04‡	2.32	2850±119.4 (7)	124§	1104.4±51.5	900±50	1.21±0.10
IM 1743−291	359.95	−0.33	~0.06‡	2.32	781.4±33.4 (8–10)	124§	212.8±14.4	400±50	0.51±0.1
A1742−297	359.4	−0.385	~0.07‡	2.32	1812.5±67.3 (7, 10, 11)	124§	657.3±29.0	600±50	1.1±0.1
GX 5−1	5.08	−1.03	2.22	2.48	449.2±18.6	144.0§	37.1±7.5	175±25	0.21±0.05
GX 13+1	13.52	+0.08	2.9	1.91	415.6±21.5	96.0§	121.6±11.1	100±10	1.21±0.2
IM1727−335	354.1	+0.6	1.03‡	1.96	235.7±18.4 (8, 9)	124.0§	−3.7±9.4	250±50	−0.02±0.05
GX 3+1	2.27	+0.8	6.01	1.55	264.0±14.0 (8, 9, 12–14)	48.0§	122.3±9.0	25±5	4.9±1.0
GX 9+1	9.07	+1.15	3.28	1.91	536.6±13.2 (8, 9, 12–15)	84.0§	196.9±6.9	75±25	2.6±0.9
GX 17+2	16.4	+1.3	5.4‡	1.62	397.8±15.8 (8, 9, 12–16)	62.0§	183.6±9.8	30±10	6.1±2.1

† From references 17 and 18.
‡ $R_\odot \approx 10$ kpc assumed.
§ For $n(\text{H I}) = 0.4$ atoms cm^{-3}.

References: 1, Watson *et al.* (1983); 2, Pye *et al.* (1984); 3, Smith *et al.* (1985); 4, Wang & Seward (1984); 5, Becker & Szymkowiak (1981); 6, Becker & Helfand (1984); 7, Proctor *et al.* (1978); 8, Jones (1977); 9, Markert *et al.* (1979); 10, Cruddace *et al.* (1978); 11, Lewin *et al.* (1976); 12, Seward *et al.* (1972); 13, Hertz & Grindlay (1984); 14, Cruddace *et al.* (1972); 15, Ecran & Cruise (1984); 16, Parsignault & Grindlay (1978); 17, Radhakrishnan *et al.* (1972); 18, Caswell *et al.* (1975); 19, Sanders *et al.* (1984); 20, Li *et al.* (1983).

strong concentration of these sources towards the Galactic Centre direction), leading to $N(\mathrm{H\,I}) = 120 \times 10^{20}$ atoms cm^{-2} for a mean H I volume density of 0.4 atoms cm^{-3} (Burton 1976). As usual, $\langle N_X \rangle$ represents the mean of the column density values quoted by various groups for power-law and thermal spectra and obtained for different observation epochs. It has been scaled down by the corresponding metallicity factor to yield $2N(H_2) = (\langle N_X \rangle / \langle M/M_\odot \rangle) - N(\mathrm{H\,I})$. A comparison of the source positions (table 4) with respect to the scale height of molecular gas in the inner Galaxy shows that essentially all the contribution to $\int T^{12} \mathrm{d}v$ along an individual line of sight is made by the gas in the Molecular Ring at $R \approx 6$ kpc. We have accordingly divided $N(H_2)$ obtained above by the entire $\int T^{12} \mathrm{d}v$ measured along the given line of sight to determine α_{20}^{+}.

Figure 8 summarizes our results, where, for the reasons just mentioned, all the α_{20}^{+} values, except those for the SNRs W44 and W49B, have been plotted at $R \approx 6$ kpc to underline that,

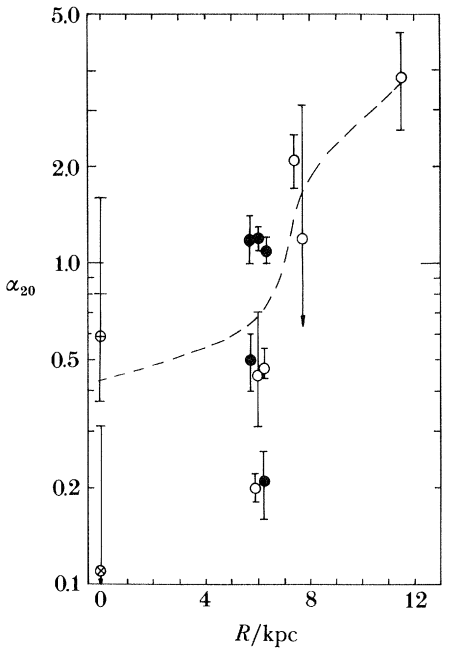

FIGURE 8. The dependence of α_{20} on the Galactocentric distance R as suggested by spectral studies of a number of X-ray sources: ○, SNRs; ●, bulge sources; ⊕, A1742−289; ⊗, Einstein G.C. sources. Three binary systems show evidence of significant circumstellar absorption and the corresponding α_{20} are not shown. A fourth source gives a negative α_{20}, presumably because of uncertainties in its $\langle N_X \rangle$ or distance estimates, or both, and this unphysical value is also not shown. It is seen that the spread in α_{20} values corresponding to $R \approx 6$ kpc is much greater than that expected on the basis of the quoted errors and this underlines the need for averaging over many values. The dotted line represents the mean α_{20} obtained thus for the sources in the figure; there is a clear suggestion of α_{20} decreasing towards the inner Galaxy, from a local value of 3.8 ± 1.4 at $R \approx 10$ kpc to *ca.* 0.7 at $R \leqslant 6$ kpc. When the above-mentioned four sources are also included, we find $\langle \alpha_{20} \rangle = 1.6$ at $R \approx 6$ kpc, which is still much smaller than the 7.2 preferred by Sanders *et al.* (paper I).

regardless of the actual Galactocentric distance (see table 2), they effectively represent α_{20}^{+} corresponding to the Molecular Ring region. Both W44 and W49B lie outside this Ring and have been plotted at their *actual* R values; they give $\alpha_{20}^{+} \approx 2.1$ with an uncertainty of *ca.* ± 2.0, mainly because N_X for W44 is not very well constrained by the currently available IPC observations (Watson *et al.* 1983; Petre *et al.* 1983; Smith *et al.* 1985). Sources GX 3+1,

GX 9+1 and GX 17+2 have been omitted from the diagram as they show evidence for circumstellar absorption. The individual α_{20}^{+} values at $R \approx 6$ kpc again show a wide scatter around an average value $\alpha_{20}^{+} \approx 0.7$, but all of them lie well below the α_{20} found locally (§3.3.3). That α_{20}^{+} at $R \approx 6$ kpc is really smaller can be independently checked by plotting $N(H_2)$ obtained for the non-SNR type sources against the corresponding $\int T^{12}\mathrm{d}v$ (figure 9); the slope of the least-square linear fit to the data gives $\alpha_{20}^{+} = 0.68 \pm 0.16$.

There is thus a strong suggestion that α_{20} should decrease as one proceeds from $R \approx 10$ kpc to $R \approx 6$ kpc in the inner Galaxy.

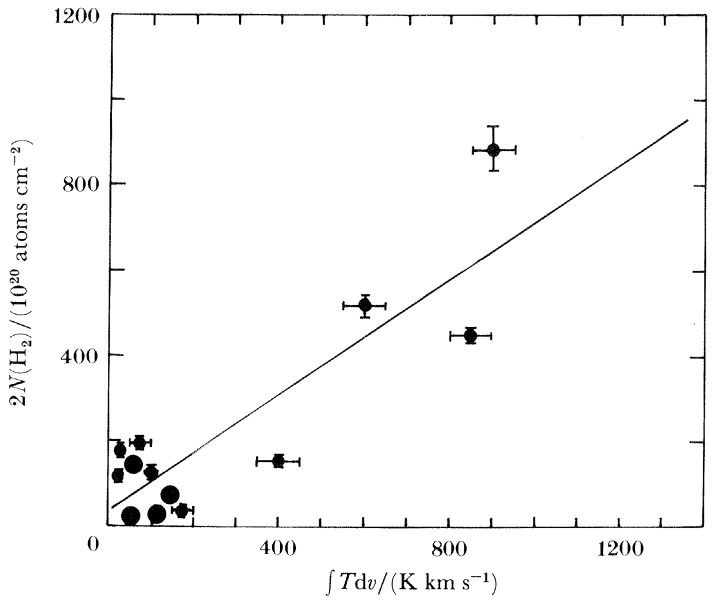

FIGURE 9. A correlation plot derived for 13 Galactic X-ray sources (some with unknown distances) between $N(H_2)$, the column density of molecular hydrogen along the line of sight, and the corresponding $\int T^{12}\mathrm{d}v$ (taken from paper I). The slope of the line yields $\alpha_{20} = 0.68 \pm 0.16$, which is likely to be a representative value for $R \approx 6$ kpc, since the line of sight to the most of these sources passes through the Molecular Ring present there.

3.3.5. α_{20} *at the Galactic Centre*

We use here XRSS that are most probably located within the Galactic nucleus (defined for our present purpose as a region of *ca.* 0.1° angular size around Sgr A West (Oort 1977). Rotating modulation collimator observations of the Galactic Centre region have helped identify here the transient source A1742−289, which is found to be located *ca.* 1′ from Sgr A West. Several groups (Proctor *et al.* 1978; Branduardi *et al.* 1976) have made spectral measurements of this source, leading to $\langle N_X \rangle = 1765 \times 10^{20}$ atoms cm^{-2}. More recently, observations with an arc-minute angular resolution by Watson *et al.* (1981), made at the Einstein Observatory, have revealed 10 point-like XRSS in the Galactic nucleus, in addition to a region of weak, diffuse emission, *ca.* 0.5° in size. All of these XRSS are marked by a lack of flux variability and the brightest one among them is positionally coincident with Sgr A West itself. The implied high number density of these sources and the fact that they roughly follow the total gas distribution in its longitudinal asymmetry (Watson *et al.* 1981; Matteson 1982; Brown & Liszt 1984) strongly suggest that they belong to the Galactic nucleus with $R = 10$ kpc. The spectral data

currently available for the sources are, unfortunately, of a rather poor quality and give $\langle N_X \rangle = (600 \pm 400) \times 10^{20}$ atoms cm^{-2}; nevertheless, they are useful.

We take $N(\mathrm{H\,I}) = 120 \times 10^{20}$ atoms cm^{-2} and $\int T^{12} \mathrm{d}v = 840$ K km s^{-1} (S.S.S.), thus assuming implicitly that half of the H I and H_2 along the line of sight to the Galactic Centre lies in front of these sources. For a metallicity factor of *ca.* 2.8 (Li *et al.* 1982), we thus obtain $\alpha_{20}^{+} = (0.59 \pm 0.04)$ for A1742−289 and (0.11 ± 0.17) for the Einstein sources.

We realize that the foregoing assumption about the distribution of H_2 can be in error because of the known clumpy nature of the molecular gas, which can allow the XRSS to be 'seen' through 'holes' present in between the molecular clouds. However, the rather large number of sources (11) that we are dealing with here would make such a possibility quite unlikely. Nevertheless, we have considered the worst possibility, where the XRSS are placed in front of the clouds in the Galactic nucleus so that the main H_2 that they 'see' is that along the line of sight at $R = 6$ kpc. This increases the value of α_{20}^{+} derived above by a factor of *ca.* 2.8 but it is still 'small'. The other extreme situation, where these sources are assumed to lie on the far side of the Galactic nucleus, would cause α_{20}^{+} to decrease by a factor of *ca.* 1.6. These limits are also indicated in figure 8.

It is evident that the X-ray data favour a value of α_{20}^{+} for the Galactic Centre, which is even smaller than that at $R = 6$ kpc.

A further reason why α_{20} must be much less than the 7.2 obtained by S.S.S. concerns the intrinsic luminosity of the X-ray sources at the Galactic Centre. With $\alpha_{20} = 7.2$, the total gas column density up to the Galactic Centre would be *ca.* 6000×10^{20} atoms cm^{-2}. Such a high column density would mean that the XRSS in the Galactic nucleus would need higher intrinsic luminosities than that generally assumed by a factor as large as *ca.* 5×10^3, and this would pose very serious constraints on the nature of these sources, as also on the processes believed to be responsible for their X-ray generation (Watson *et al.* 1981).

3.3.6. *Conclusion from the X-ray method*

Spectral studies of Galactic XRSS have been shown to yield reliable column densities of interstellar gas in situations where estimates can also be obtained from optical extinction. These studies suggest that $\alpha_{20} = 3.8 \pm 1.4$ locally ($R = 10 \pm 1$ kpc), and that α_{20} decreases towards the inner Galaxy and assumes an average value of 0.7 ± 0.2 around the Molecular Ring ($R \approx 6$ kpc). Finally, α_{20} continues to be small at the Galactic Centre, the mean value being as low as *ca.* 0.4.

3.4. *Virial theorem estimate*

3.4.1. *The principle of the virial mass technique*

The virial theorem is extensively used to give a measure of the mass of astronomical objects and molecular clouds are no exception. The usefulness of the technique stems from its apparent simplicity, requiring only a measure of the size and velocity spread of the material in the cloud, as also its insensitivity to the assumptions that go into the interpretation of the molecular emission lines. For these reasons, virial masses of clouds are widely quoted in the literature.

An accurate virial mass estimate can only come from a detailed knowledge of the structure and the internal dynamics of the molecular clouds under consideration. Such knowledge is not generally available, so one is forced to make simplifying assumptions, such as considering

spherical clouds with a simple radial dependence of density. The virial mass then follows from the expression:

$$M = kR\Delta V^2_{\mathrm{FWHM}}, \tag{5}$$

where M is the cloud mass in solar masses ($M_\odot$), R is its radius in parsecs and ΔV_{FWHM} is the line width in kilometres per second.

For a uniform density sphere k is 210, whereas if $\rho(r) \propto 1/r$ then $k = 190$.

The difficulty in applying (5) to molecular clouds arises from the need to decide which molecular lines to use to measure R and ΔV. If one uses the $J = 1 \rightarrow 0$ transition of ^{12}CO, it is likely that, owing to optical depth effects, the measured width may be much greater than the true dynamical line width. On the contrary, if one uses a rarer but optically thin line such as that from ^{13}CO, it is not immediately clear that the full extent of the cloud can be seen. The observed widths of ^{12}CO and ^{13}CO lines are significantly different and which of the two is appropriate depends on the line formation process, a process that is not well understood. In the micro-turbulent model of Leung & Liszt (1976), it is the optically thin lines that measure the velocity dispersion. This can be seen by comparing the true velocity dispersion (for their model this quantity is $\pi^{\frac{1}{2}}\Delta\nu_{\mathrm{d}}$) with that observed in the ^{12}CO and the ^{13}CO lines. Inspection of table 1 from Leung & Liszt (1976) shows that the ^{13}CO lines yield a velocity dispersion $1.8\,\Delta\nu_{\mathrm{d}}$ where the ^{12}CO lines can range up to $4.1\,\Delta\nu_{\mathrm{d}}$. Use of the latter would lead to an overestimate of the cloud mass by a factor of five, if (5) were adopted.

Similarly, Martin *et al.* (1984) have devised a clumpy cloud model in which the line profiles are formed by the variation of the beam filling factor with velocity. In their notation, the expected value for $\Delta V_{\mathrm{FWHM}} = 0.94\sigma$, whereas the measured lines yield $\Delta V(^{13}\mathrm{CO}) \approx 1.0\sigma$ and $\Delta V(^{12}\mathrm{CO}) \approx 1.4$–$1.9\sigma$ (see their figure 6).

In view of the foregoing model predictions we should adopt the ^{13}CO line widths as reflecting a realistic intrinsic velocity spread. But it needs to be borne in mind at the same time that there are other models where a velocity–density correlation exists such that the high-velocity wings of the ^{12}CO line originate in a much lower-density gas. In such a situation it is likely that the corresponding ^{13}CO line will not be excited and a narrow line width will be seen. This would not require the use of ^{12}CO line width, however, for the following reason. The velocity–density correlation arises naturally in collapse models that assume that the cloud collapse velocity varies with its size R as *ca.* R^β, with $\beta > 0$. The line wings are then formed in the low-density outer parts of the clouds. Application of these models to the actual molecular clouds, however, generally demands that $\beta < 0$, i.e. the line wings are formed in the denser parts of the cloud (Loren *et al.* 1974; Lada 1976). The virial formula itself must then be modified if the cloud is collapsing, e.g. in the extreme free fall case the cloud mass would need to be halved.

Considering all the possibilities it seems most likely that the width of the ^{12}CO line is broadened by optical depth effects and should not, therefore, be used as a measure of the dynamical velocity spread; the ^{13}CO lines should be used instead.

3.4.2. *Derivation of the line widths*

Stark (1979) has tabulated data on clouds in the Molecular Ring from observations of three fields, each approximately 1° square sampled every other beam in the $J = 1 \rightarrow 0$ transition of ^{13}CO. These data are shown in figure 10 together with the best fit line (heavy solid line),

$$\Delta V_{\mathrm{FWHM}} = (1.8 \pm 0.4)\, D^{0.21 \pm 0.06}, \tag{6}$$

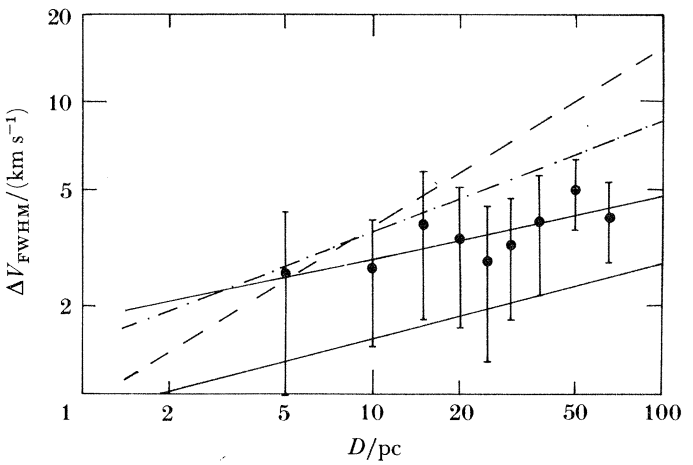

FIGURE 10. Velocity width plotted against cloud diameter for various cloud samples. Dot–dashed line, Larson, $\Delta V = 1.5L^{0.38}$; broken line, S.S.S., $\Delta V = 0.88D^{0.62}$; lower solid line, Myers, $\Delta V = 0.82L^{0.27}$ (for $L < 20$ pc); upper solid line, best fit, $\Delta V_{\mathrm{FWHM}} = (1.8 \pm 0.4)\, D^{0.21 \pm 0.06}$.

where ΔV is in kilometres per second and D is in parsecs. This may be compared with the relation

$$\Delta V_{\mathrm{FWHM}} = 0.88 \pm 0.16 D^{0.62 \pm 0.05}, \tag{7}$$

derived by Sanders *et al.* (1985) from a sample of clouds observed in the $J = 1 \rightarrow 0$ line of ^{12}CO. Before a direct comparison can be made, however, it is important to consider the possibility that there are systematic differences between the two relations owing to the different approaches used to measure D and ΔV. For ^{12}CO, the two cloud quantities measured are (i) the chord size in latitude (at constant longitude) to the 2 K km s^{-1} boundary and (ii) the mean velocity full width at half maximum measured along the chord. For ^{13}CO, similarly, the quantities plotted are (i) the mean diameter of the cloud boundary that follows the 0.4 K km s^{-1} contour and (ii) the full width at half maximum of a gaussian fit to the peak antenna temperature.

Adopting a value of 5.5 for the ratio $\int T^{12}\mathrm{d}v / \int T^{13}\mathrm{d}v$ (S.S.S.), the cloud boundary mentioned above for the ^{13}CO data will correspond to a level of 2.2 K km s^{-1} for ^{12}CO. Stark & Blitz (1978) have argued that, for local clouds, a level of *ca.* 2.6 K km s^{-1} is a good measure of the true extent of the clouds. Similarly, Sanders *et al.* (1985) have argued that if they changed their temperature cut-off from 2 K to 1 K, the cloud lengths they measure would increase only by 10–20%. If, therefore, the same sample of clouds were measured by these techniques, it seems unlikely that the measured sizes would differ by more than 20%.

Turning to the measurements of the velocity widths, there may indeed be a systematic difference between the ^{12}CO and ^{13}CO results, but it is probably in the sense that would accentuate the differences rather than decrease them. This arises because the ^{13}CO velocity width is measured at the peak antenna temperature whereas velocity widths generally decrease away from the peak (Leung & Liszt (1976). The velocity width at the peak is therefore likely to be an overestimate of the corresponding average over the whole cloud. Because it is not possible to quantify this overestimate from the available data, we have therefore adopted the line width at the peak to represent an upper limit to its true dynamical value.

The fact that the line widths measured in ^{13}CO and other optically thin transitions are much narrower than those of ^{12}CO is, of course, well known; for example, Leung & Liszt (1976) quote

that typically $\Delta V_{13} = 0.6\Delta V_{12}$, where the subscripts 12 and 13 refer to ^{12}CO and ^{13}CO respectively. With regard to absolute values, Stark & Blitz (1978) give $\Delta V_{\mathrm{FWHM}} = 4$ km s^{-1} for an optically thin line, measured some 50 pc from the cloud centre, whereas Liszt *et al.* (1981) quote $1 \leqslant \sigma_V \leqslant 2$ km s^{-1} for isolated ^{13}CO features, corresponding to $\Delta V_{\mathrm{FWHM}} = 1.4$–$2.7$ km s^{-1} for a gaussian line. Several other authors have also derived relations between ΔV_{FWHM} and D for optically thin lines. Larson (1981) obtained $\Delta V_{\mathrm{FWHM}} = 1.5D^{0.38}$ over a wide range of cloud sizes, and Myers (1983) found $\Delta V_{\mathrm{FWHM}} = 0.82D^{0.27}$ for sizes up to *ca.* 20 pc. These relations bracket that deduced from Stark's data.

The differences between the relations between ΔV_{FWHM} and D for the ^{12}CO and ^{13}CO lines are therefore real. Not only are the ^{13}CO lines narrower but the discrepancy with the line widths of ^{12}CO increases as the cloud diameter increases.

This has an important effect on the derived cloud mass distribution and we shall return to this point later.

The reason for the more rapid increase in ΔV_{FWHM} with D for the ^{12}CO line compared with that for the ^{13}CO line is not known. For a simple model in which the optical depth is proportional to D, the relation for ^{12}CO should be steeper by *ca.* $D^{0.1}$ than that for ^{13}CO, provided we assume that ^{13}CO reflects the true intrinsic velocity spread. Simple optical depth effects would therefore seem to be ruled out. A likely possibility is that the ^{12}CO data are affected by blending (Liszt & Burton 1981; Liszt *et al.* 1981), although Sanders *et al.* (1985) point out that their technique of measuring clouds at constant velocity eliminates most of the blending.

3.4.3. *Application to the estimation of cloud masses*

The various relations between ΔV_{FWHM} and D are given in table 5 together with the resulting virial mass formulae. Most of the differences arise through taking the values for the ^{12}CO or ^{13}CO lines. There is also some effect because of the difference in the values of k adopted in the virial theorem. We have used here $k = 190$, whereas Sanders *et al.* prefer $k = 260$. This in turn is due to our use of a constant velocity dispersion throughout the model cloud whereas Sanders *et al.* adopt a smaller dispersion in the denser cloud core.

TABLE 5. SUMMARY OF THE VARIOUS VIRIAL THEOREM ESTIMATES PRESENTED IN THE TEXT AND THE ASSUMPTIONS USED IN THEIR DERIVATION

(In all cases the units are: M, $M_\odot$; D, parsecs; ΔV, kilometres per second.)

virial formula	$\Delta V = f(D)$	k	α	reference
$M = 308D^{1.42}$	$\Delta V = 1.8D^{0.21}$	190	$1.3^{+1.7}_{-0.8}$	see text (equation (6))
$M = 101D^{2.24}$	$\Delta V = 0.88D^{0.62}$	260	9.2	Sanders *et al.* (1985)
$M = 214D^{1.76}$	$\Delta V = 1.5D^{0.38}$	190	$3.1^{+1.2}_{-0.9}$	Larson (1981)

Armed with the above relation between the cloud mass and its size, an estimate can be made for the average α_{20} for the whole Galaxy by way of a determination of the total gas mass in the Galaxy. This requires a knowledge of $N(D)\,\mathrm{d}D$, the number of clouds with diameters between D and $D + \mathrm{d}D$. The available data are not sufficient to determine $N(D)$ uniquely, but, making the usual assumption of a power-law dependence, $N(D) \propto D^{-\gamma}$, lead to best fit values of γ in the range 2.3–3.3.

To ensure that uncertainties in $N(D)$ do not obscure the major difference in total galactic

gas mass, we have used $N(D)$ as given by Sanders *et al.* (1985) throughout. It is found that the total gas mass is up to a factor 7.2 smaller than derived by Sanders *et al.*, yielding in turn $\alpha_{20} = 9.2/7.2 = 1.3$ (see table 5). In so far as most of the molecular gas outside the Galactic nucleus ($R \geqslant 500$ pc) resides in the Molecular Ring at $R \approx 6$ kpc, this value of α_{20} would then essentially refer to that region.

Another important consequence of using (8) is to steepen the cloud mass spectrum to $N(M) \propto M^{-1.92}$, rather than $M^{-1.58}$, as obtained by Sanders *et al.* ($N(M)\,\mathrm{d}M$ represents the number of clouds with masses between M and $M+\mathrm{d}M$). Also, when we ask about the cloud size such that clouds greater than this size contain 50% of the total mass, we find that $D = 41$ pc rather than the 48 pc given by the virial theorem when applied to the ^{12}CO line. In preceding sections we have presented evidence that α_{20} decreases in the inner Galaxy. Further, supporting evidence can be found here in the differences in the relation between ΔV_{FWHM} and D obtained from the data of Larson (1981) and from Stark (1979).

From Larson's data with $\gamma = 2.3$, clouds with $D > 44$ pc contain 50% of the Galactic gas mass, $N(M) \approx M^{-1.74}$ and $\alpha_{20} = 3.1$. The latter is compatible with Larson's own implied value of α_{20}, because he uses $^{13}\mathrm{CO}/\mathrm{H}_2 = 2 \times 10^{-6}$, which, following the discussions of S.S.S. on the use of Local Thermodynamic Equilibrium (LTE), gives $\alpha_{20} = 3.6$. The small difference between our value (3.1) and that of Larson (3.6) arises because we have assumed the virial theorem to hold and have thus used ΔV and D to calculate M, whereas Larson used the cloud masses as derived by molecular lines to verify that the clouds were in approximate virial equilibrium.

The errors on the estimates due to the uncertainties in the relation between ΔV_{FWHM} and D are, for Stark's data $\alpha_{20} = 1.3^{+1.7}_{-0.8}$, and for Larson's $\alpha_{20} = 3.1^{+1.2}_{-0.9}$. Proceeding for the moment on the assumption that the differences are real we note that the bulk of Larson's data arises from regions within 1–2 kpc of the Sun, whereas the bulk of Stark's clouds lie in the Molecular Ring at $R = 5$–6 kpc suggesting that α_{20} decreases in the inner Galaxy.

However, there is also the possibility that the difference in α_{20} values may be caused by the different selection techniques used to compile the samples. Thus, specifically, Larson (1981) does not exclusively use data from ^{13}CO and also most of the weight in his fit comes from cloud regions with $D < 10$ pc, whereas most of Stark's measurements belong to $D > 10$ pc. To remove these uncertainties in the interpretation it is necessary to await future data involving larger and more homogeneous cloud samples.

It has been argued (S.S.S.) that the virial theorem supports values of α_{20} as large as 9.2. This result is dependent on the assumption that the ^{12}CO line width is a good measure of the dynamical line width. This is clearly not so in many cloud models where the ^{12}CO line is broadened by optical depth effects. Use of the more appropriate optically thinner lines gives values of α_{20} smaller by a factor 3 locally, with some evidence of even smaller values in the inner Galaxy.

3.5. *The galaxy-count technique*

3.5.1. *Principle*

For a known gas:dust ratio, the 'galaxy count', the number of galaxies seen per square degree along a given line of sight, can be used to determine the column density of total gas, $N(\mathrm{H_t})$, in that direction (Mihalas & Binney 1981). This technique has recently been used successfully (Strong & Lebrun 1982; Strong *et al.* 1982) to trace the high-latitude ($|b| \geqslant 10°$)

gas. Here we shall discuss a new variant of this technique, which we have found useful for estimating $N(H_t)$, and hence α_{20} locally, both in the anticentre direction ($l = 140$–$240°$, $|b| \leqslant 20°$) and towards the inner Galaxy ($l = 15$–$100°$, $b = 4$–$10°$). We start by using the galaxy count data of Kiang (1968) and define a parameter ϕ, which, for a given region of the sky, is the ratio of the number of square degree bins with zero galaxies to the number of bins with a non-zero galaxy count. It is important to note that the angular size of the sampled region should be sufficiently large to reduce the statistical error on ϕ. Fortunately, this constraint is satisfied quite well by several high-latitude molecular clouds in the Galaxy. An advantage of the parameter ϕ is that it is less sensitive than the usual method to the fluctuations in $\int T \mathrm{d}V$ in the field of view, i.e. to the clumpiness of the clouds.

An important requirement now is to show that ϕ is a good measure of $N(H_t)$. For this purpose we shall first refer to the outer Galaxy ($l = 140$–$240°$, $|b| \leqslant 10°$), since essentially all the gas here exists as H I and is reliably mapped through the 21 cm line measurements (Weaver & Williams 1971; Riley *et al.* 1983). Using Kiang's listing we have determined ϕ for the different mean H I column densities, $\langle N(\mathrm{H\,I}) \rangle$ that are encountered in this region and have plotted one against the other in figure 11. In recognition of what has been said above about essentially all the gas in the outer Galaxy being in atomic form, we have represented the abscissa in the figure by the total gas column density $N(H_t)$. The line labelled 'anticentre' passes through most of the data points and should therefore reflect the variation of ϕ with $N(H_t)$; it is

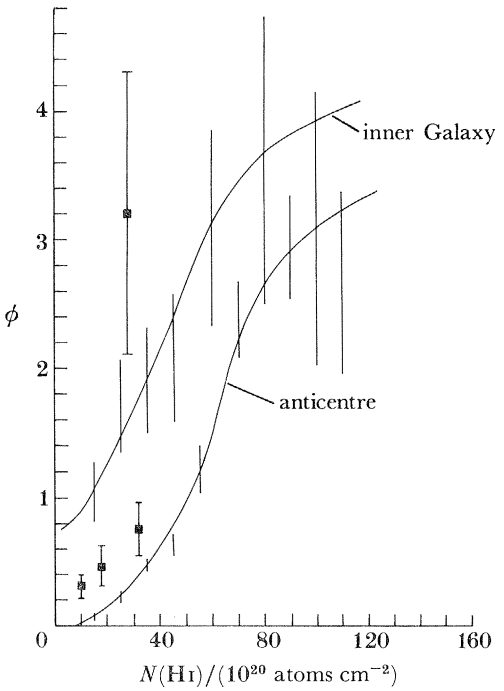

FIGURE 11. The parameter ϕ, which is a measure of optical extinction (see text for details), plotted as a function of $N(\mathrm{H\,I})$, the column density of the atomic hydrogen as given by the 21 cm radio data. The full curves represent datum lines for the anticentre direction ($l = 140$–$240°$, $|b| < 10°$) and for the inner Galaxy ($l = 15$–$100°$, $|b| = 4$–$10°$); interestingly, the lines have the same form but are laterally displaced, presumably because the dust:gas ratio is higher in the inner Galaxy. The positions of some known molecular clouds are also shown in the figure: 1, Taurus 1; 2, Orion; 3, Taurus 2; 4, $l = 20$–$35°$, $b = 4$–$10°$. The corresponding column densities of H_2 are given by the 'distances' by which these points need to be transposed horizontally to reach the respective line. This method provides an independent determination of α_{20} locally: (2.7 ± 0.5).

evident that ϕ increases more rapidly in the beginning but more slowly beyond $N(\mathrm{H_t}) \approx 8 \times 10^{21}$ atoms cm^{-2}.

It is not our purpose here to explain this shape of the datum line, though, in passing, it can be mentioned that it can either reflect a genuine change in the dust:gas ratio for $N(\mathrm{H_t}) \approx 8 \times 10^{21}$ atoms cm^{-2} or, more plausibly, that the dust closer to the Galactic plane, where $N(\mathrm{H_t})$ is larger, is not homogeneously distributed, thereby facilitating galaxies to be seen through 'holes' between the dust clumps.

Figure 11 also shows a second curve labelled 'inner Galaxy'. This is the datum line that we obtained for $l = 15$–$100°$ and $|b| \leqslant 10°$ by plotting ϕ against $\langle N(\mathrm{H\,I}) \rangle$ for only those angular bins ($\Delta l = 5°$, $\Delta b = 1°$) for which a recent low-resolution ^{12}CO survey by Dame (1984) gives $\int T^{12} \mathrm{d}v < 3$ K km s^{-1}, implying an essential absence of molecular gas along these directions. Interestingly, although this datum line has more or less the same form as that for the anticentre, we find it lying consistently above the latter curve, even for the smallest measured $N(\mathrm{H_t}) \approx 1.5 \times 10^{21}$ atoms cm^{-2}. Whereas this could possibly mean that there is some extra dust in the direction of the small l which has negligible gas associated with it, it also highlights the need for using molecular clouds belonging to the first and (second + third) quadrants.

3.5.2. *Results*

Table 6 lists $N(\mathrm{H\,I})$ for the molecular clouds in the Orion and Taurus complexes, and for an apparent conglomerate of high-latitude ($b = 4$–$10°$) clouds mapped by Dame (1984) in the first quadrant between $l = 20$ and $35°$. The corresponding ϕ for these cloud regions deduced from Kiang (1968) are also listed in table 6, as are their average $\int T^{12} \mathrm{d}v$ and $N(\mathrm{H\,I})$ values obtained from Dame (1984) and Weaver & Williams (1971) respectively.

TABLE 6

H_2 clouds	b range (deg)		l range (deg)	$\langle \int T \mathrm{d}v \rangle$ (K km s^{-1})	ϕ	$N(\mathrm{H\,I})$ (10^{20} atoms cm^{-2})	$N(\mathrm{H_t})$ (10^{20} atoms cm^{-2})	α_{20}
Orion (A+B)	−12	−20	204–216	5.2	0.46±0.14	18.1	33±5.5	2.9±1.0
Taurus 1	−13	−24	157–177	7.1	0.31±0.09	10.2	27±4.5	2.4±0.6
Taurus 2	−6	−12	156–170	5.2	0.76±0.21	23.0	43±6.5	3.8±1.3
inner Galaxy	4	10	20–35†	15.2†	3.2±1.1	28.1	92±18	4.2±1.2

† Only $\int T \mathrm{d}v \geqslant 10$ K km s^{-1}.

In figure 11 we have plotted ϕ for these regions against the respective $\langle N(\mathrm{H\,I}) \rangle$ along the line of sight; as expected, the points for the Orion and the Taurus clouds line above the anticentre datum line and that for the cloud complex in the first quadrant similarly lies above its corresponding datum line, suggesting that the extra extinction is caused by the dust associated with the molecular gas in these clouds. Obviously, then, the column density of this gas, $N(\mathrm{H_2})$, is given by the 'distance' by which each point needs to be transposed horizontally (constant ϕ) to reach the corresponding datum line. $N(\mathrm{H_2})$ values obtained thus are also given in table 6 along with the corresponding α_{20} values that follow. It is evident that, within the quoted errors, all these values are mutually compatible and lead to a weighted average $\alpha_{20} = 2.7 \pm 0.5$. This is close to the values obtained for the local α_{20} by other techniques described here and in paper I. It may be noted that because of the uncertainty in the exact

PHILOSOPHICAL TRANSACTIONS OF THE ROYAL SOCIETY A MATHEMATICAL, PHYSICAL & ENGINEERING SCIENCES

shape of the datum curve for high column densities (*ca.* 10^{22} atoms cm^{-2}), we have not been able to use this technique for finding α_{20} for the inner Galaxy at lower latitudes ($|b| < 4°$).

3.6. *Infrared estimates of α_{20} for the inner Galaxy*

Unlike in the optical region, the extinction by the interstellar dust at near-infrared (NIR) wavelengths is sufficiently small to enable us to look deep into the inner Galaxy, even including the dense Galactic nucleus. By examining the degree of reddening suffered at these wavelengths, an estimate can be made of the gas column density along various directions under the assumption of a large-scale uniformity in the Galactic dust:gas ratio. As discussed below, this can yield independent estimates of α_{20} in the inner Galaxy, both at the position of the 6 kpc H_2 ring and at the Galactic Centre (G.C.). It needs to be mentioned, however, that there are two main areas of potential uncertainty in the application of this otherwise simple method (Greenberg & Hong 1974; Savage & Mathis 1979): (i) the need for an unreddened comparison star or a galactic nucleus source with identical intrinsic energy distribution, and (ii) the exact shape of the extinction curve, particularly at the infrared wavelengths. In what follows, therefore, we shall adopt a line that represents the contemporary majority opinion.

3.6.1. α_{20} *at* $R \approx 6$ kpc

Several groups (Okuda *et al.* 1979; Hayakawa *et al.* 1981; Matsumoto *et al.* 1982) have recently carried out low-resolution NIR balloon surveys of the inner Galaxy along the Galactic plane ($|b| < 0.5°$). If we exclude their data for $l \approx 0°$, to remove the G.C. contribution, we can find the average column density of the total gas along a line of sight that passes through the 6 kpc Molecular Ring. Following the arguments advanced in the X-ray method, the value of α_{20} that we shall derive in the process will effectively correspond to $R \approx 6$ kpc. Following Okuda *et al.* (1979), the average extinction at 2.4 μm for $|l| = 1$–$6°$ is $\langle A_{2.4} \rangle = 1.7 \pm 0.5$. These authors prefer $A_v/A_{2.4} = 12.4$, so that the total visual extinction at 0.55 μm is given by $A_v = 21.1 \pm 6.2$ for $\langle l \rangle \approx 2.5°$. This gives a column density of total gas, $N(H_t) = (400 \pm 120) \times 10^{20}$ atoms cm^{-2} (Bohlin *et al.* 1978). Using the value of Burton (1976) for the average column density of atomic hydrogen in the corresponding (l, b) range, $N(HI) \approx 150 \times 10^{20}$ atoms cm^{-2}, the expected column density of H_2 follows as $2N(H_2) \approx 250 \pm 60 \times 10^{20}$ atoms cm^{-2}. From S.S.S., we obtain for this region $\int T^{12} dv = 194.2 \pm 5.7$ K km s^{-1}, and hence $\alpha_{20} = 1.3 \pm 0.3$ at $R \approx 6$ kpc.

Matsumoto *et al.* (1982) quote an average visual extinction $\langle A_v \rangle = 15 \pm 4$ magnitudes after excluding the G.C. contribution. This yields $\alpha_{20} = 0.7 \pm 0.2$. More recently, Eaton *et al.* (1984) have made star counts at 2.2 μm in the Galactic plane along several directions with l between 0 and 60° and have attempted to fit the observed extinction characteristics with a reasonable model. They find that, for l away from the G.C., the best fit form for the extinction is roughly uniform with a value of *ca.* 0.1 mag kpc^{-1} at 2.2 μm. Since the extinction at this wavelength is between 0.10 and 0.13 of that at 0.55 μm (Savage & Mathis 1979; Gatley 1982), we should expect a total visual extinction $A_v = 20$–25 mag over the entire path through the Galaxy for $\langle l \rangle \approx 2.5°$, in reasonable agreement with the results of Okuda *et al.* (1979) and Matsumoto *et al.* (1982).

3.6.2. α_{20} *at the Galactic Centre*

There is general agreement now that the NIR from the Galactic nucleus is predominantly of stellar origin (Matsumoto *et al.* 1982; Oort 1977; Spinrad *et al.* 1971) and that the estimates

of A_v derived by comparing the observed G.C. reddening with the nucleus of M31 should be reliable. The values often quoted in the literature in this connection are based on the ground-based, high-resolution observations at 1.65, 2.2 and 3.4 μm by Becklin & Neugebauer (1968), and by Spinrad *et al.* (1971), at the somewhat shorter wavelengths of 1.06 and 1.18 μm. A comparison of the observed Galactocentric fluxes at these wavelengths by Spinrad *et al.* (1971) yields a total visual extinction between the Sun and the G.C. having a mean value $\langle A_v \rangle_{G.C.} = 29.3 \pm 2.2$ mag, to be compared with $(A_v)_{G.C.} \approx 30$ mag deduced by Okuda *et al.* (1977) from their 2.4 μm mapping of the G.C. region. If we assume a uniform dust:gas ratio and also that the composition and the size of the scattering grains are the same as those found locally (an *ad hoc* assumption, but quite extensively used nevertheless), we can use the Bohlin *et al.* (1978) relation (equation (2)) to obtain the column density of total gas up to the G.C. For the above value of $\langle A_v \rangle_{G.C.}$, we then find $N(H_t) = 550 \pm 40 \times 10^{20}$ atoms cm^{-2}. The corresponding N(HI) is 120×10^{20} atoms cm^{-2} (Burton 1976) and $\int T^{12} dv = 850$ K km s^{-1} (S.S.S.), leading to $(\alpha_{20})_{G.C.} = (430 \pm 20)/850 = 0.5 \pm 0.03$, in excellent agreement with that obtained earlier (§3.3.4).

In passing, we should also like to mention that a lower limit of $(A_v)_{G.C.} \approx 5$–15 mag has been inferred (Greenberg & Huang 1974) whereas, in the other direction, Aitken & Jones (1973) adopt a value as high as 75 magnitudes. With the other assumptions taken to be unchanged, these values of $(A_v)_{G.C.}$ correspond to $(\alpha_{20})_{G.C.}$ between the limits 0.1–1.5, again not inconsistent with the X-ray and γ-ray results, but far below the conventional 2.6 mm ^{12}CO value used to derive the H_2 mass at the G.C.

4. The inferred mass of gas in the Galaxy

4.1. *Surface density of gas as a function of R*

Figure 12 shows the derived values of α_{20} plotted as a function of R. Where plotted, the error bars reflect only the statistical uncertainties in the plotted points. These data indicate that α_{20} locally lies in the range 2–4. Systematic effects would, of course, allow values of α_{20} outside this range; indeed, much larger values of α_{20} have been advocated, based on different analyses of the same data sets as we have used here. Our arguments against these large values of α_{20} are detailed in the preceding sections. A straight average of the data points in figure 12 gives $\alpha_{20} = 3.0$ locally, consistent with our previous analysis (paper I).

In the inner Galaxy, specifically in the Molecular Ring, the scatter in α_{20} is much larger, reflecting the additional difficulty of calibrating the $N(H_2)$ against $\int T^{12} dv$ relation in distant regions. Owing to this large scatter the interpretation of the data is more ambiguous. A straight average of the values plotted gives $\alpha_{20} = 1.8$ indicating a fall in α_{20} in the inner Galaxy although a constant α_{20} is just compatible with the data.

Turning to the Galactic Centre region, this shows a clear decrease in α_{20} relative to the locally determined value, as pointed out previously (Bhat *et al.* 1984; paper I; and independently by Blitz *et al.* 1984). Taken as a whole the data are therefore either compatible with a steady decrease in α_{20} towards the Galactic Centre or a constant value outside $R = 0.5$ kpc with a value smaller by a factor *ca.* 6 at the Galactic Centre. We prefer the former situation but in any event the detection of at least one region of the Galaxy where substantial variations in α_{20} occur is a powerful argument against the application of the local calibration of α_{20} to the bulk of the Galactic CO.

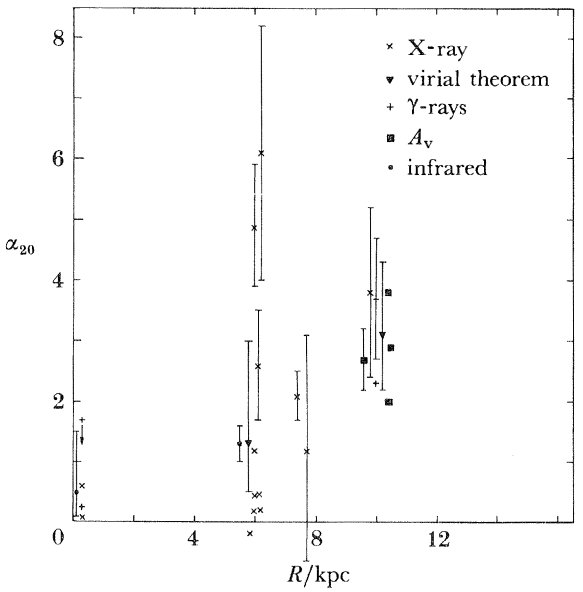

FIGURE 12. Summary of estimates of α_{20} as a function of Galactocentric radius. The binary sources omitted from figure 8 have been included here.

In paper I we attributed the decrease in α_{20} to the increase in metallicity (specifically the O/H ratio) observed in the inner Galaxy. However, there are arguments, both theoretical (see, for example, Kutner & Leung 1985) and observational (Young *et al.* 1985), that metallicity as defined cannot be a major influence on the CO–H_2 conversion factor. In §6 we discuss the observational constraints on a metallicity-dependent α and here discuss other possible causes of a decrease in α_{20} in the inner Galaxy.

In a recent review, Williams (1985) discusses, from the point of view of interstellar chemistry, the influences on the CO:H_2 ratio. It is clear that this ratio is a sensitive function of many poorly known molecular cloud properties and is likely to vary considerably even within a single molecular cloud. In global surveys averaging over large regions of the Galactic plane it may be that the adoption of a constant α_{20} is justified provided, of course, that the mean cloud properties are not a function of R. Williams (1985) puts forward the interesting suggestion that non-equilibrium chemistry is needed to explain the abundances of molecular species in molecular clouds and that shocks in the ISM control the gas-phase abundances of metals. If this is so then the postulate of stronger and more frequent shocks in the inner Galaxy could simulate a metallicity effect. The important point here is that local determinations of the fraction of carbon tied up in CO yield *ca.* 15%, so there is a large potential reservoir of carbon that could increase the CO:H_2 ratio if it could be released into the gas phase.

Opposing such shock disruption is accretion onto grain surfaces. This raises the possibility that in quiescent clouds a large fraction of the CO could be on grain surfaces, making them undetectable via CO emission. This could well have important consequences for the amount of gas in the outer Galaxy (i.e. the present estimates of $M(H_2)$ in this region could be gross underestimates).

Kutner & Leung (1985) have proposed that temperature is the dominant factor in determining α_{20} and that $\alpha_{20} \approx T_K^{-1.3}$. Their results suggest $\alpha_{20} = 4$ for the GMC envelopes in

the Molecular Ring with the proviso that this may yield a total mass too high by a factor 2 if there are many sources of local heating in the clouds. If the clouds in the inner Galaxy are hotter than the clouds in the outer Galaxy, as claimed by Kutner & Mead (1981), then α_{20} should fall as one proceeds towards the Galactic Centre, as we prefer.

The data from Frerking *et al.* (1982) on the ρ Oph cloud is consistent with $\alpha_{20} \approx T_K^{-1.3}$, whereas that on Taurus shows no such correlation. If substantiated, however, this result would have a significant influence on the CO-inferred H_2 masses in the Galactic Centre, where much higher cloud temperatures are found giving results more compatible with estimates in other wavebands. It would also complicate the interpretation of the azimuthal variations in H_2 density because it has been suggested that the hotter molecular clouds show arm-like spiral structure (Sanders *et al.* 1985).

If there are indeed differences in the mean cloud properties as a function of R then it should be possible to detect these by comparisons of observations in both ^{12}CO and ^{13}CO. This has been attempted by several groups with contradictory results. Solomon *et al.* (1979) found that the ratio of ^{12}CO to ^{13}CO emissivity in the northern hemisphere was at best only weakly dependent on the Galactocentric radius. A similar conclusion was reached by Sanders (1981) for the southern hemisphere. Sanders's (1981) data is such that the weak dependence, if present, is in the sense that the emissivity ratio decreases on either side of the Molecular Ring. Liszt *et al.* (1984) found a strong dependence of the ^{12}CO to ^{13}CO emissivity ratio on R in the sense that this ratio increased on either side of the Molecular Ring with variations of a factor of 2 across the Galactic disc. The variation is in accordance with expectation for a metallicity effect, although the increase in the ratio inside the Molecular Ring would argue against a smooth increase in metallicity up to the Galactic centre. Liszt *et al.* (1984) argue that their result is more probably due to a variation of the mean cloud column density than to a metallicity effect.

The apparent discrepancy between these results may be related to the different longitude samplings employed. The more widely spaced longitude sampling of Solomon *et al.* (1979) and Sanders (1981) will tend to wash out any azimuthal variations in the emissivity ratio compared with the more restricted (in longitude) but more finely spaced data of Liszt *et al.* (1984). This could be important since as already mentioned, the hotter molecular clouds may be associated with spiral structure.

There are therefore several mechanisms that could cause a decrease in α_{20} in the inner Galaxy, but the observational evidence in favour of any of them is ambiguous.

Rickard & Blitz (1985) have also pointed out that metallicity and heating act in opposite senses on the ^{12}CO:^{13}CO emissivity ratio and that small observed changes may represent large changes in the CO–H_2 conversion factor. In view of the evidence presented above, however, (figure 12) we shall pursue the interpretation that α_{20} steadily decreases in the inner Galaxy. Although the best dependence of α_{20} on Galactocentric radius is not clear, we have adopted an exponential form to facilitate comparison with other Galactic distributions; the decrease adopted is 0.06 dex kpc^{-1}, corresponding to a scale length of 8 kpc.

Applying this decrease to the data in figure 4, $M(H_2)$ follows as: $6.1 \times 10^8\ M_\odot$ for $R = 0.5$–10 kpc. This value is similar to that in paper I owing to our somewhat larger values of α_{20} being offset by a reduction by a factor 1.3 in line with the discussion in §2. If instead we assume $\alpha_{20} = 3.0$ everywhere then $M(H_2) = 9.8 \times 10^8\ M_\odot$.

We have not applied these values of α_{20} to the CO distribution of Dame (1984) because the bulk of the calibration data are taken from large-dish observations (and Dame used a small

dish). Until the differences between the data in figures 1 and 4 are reconciled it is inevitable that α_{20} will be a function of the survey data used.

The Galactic Centre region shows clear evidence for a much smaller α_{20}, as we have remarked already and as is discussed in detail in Bhat *et al.* (1984). The best estimate, for $R < 0.5$ kpc, given in that paper is $2 \times 10^7\ M_\odot$ of molecular hydrogen. Adding in helium and heavier atoms the best estimate of the mass is $3 \times 10^7\ M_\odot$ with an upper limit of $9 \times 10^7\ M_\odot$.

5. Implications of the lower estimates of gas mass

5.1. *Galactic evolution*

These are the subject of detailed current study but some preliminary comments can be made here.

Perhaps the most obvious consequence is that, in so far as stars form mainly from dense molecular clouds, the efficiency of star formation must be higher than previously thought. Detailed recent work by Rana & Wilkinson (1985) has enabled an evolutionary model to be deduced that fits the new gas distribution and has certain attractive features, in that it avoids the need for gas infall and also offers a possible solution of the 'G-dwarf problem'.

5.2. *The Oort cloud of comets*

A number of calculations have been made for the probability of the Oort cloud of comets being stripped by interactions with GMC and, with the conventional mean cloud masses, it appears that this stripping should be essentially complete in the lifetime of the Solar System (Clube & Napier 1982; Napier & Staniuchi 1982).

Following the more recent analysis of Bailey (1983), in which the stripping mechanism is discussed in great detail, we find that with the reduced mean cloud mass locally (specifically, a median mass of $1.3 \times 10^5\ M_\odot$ compared with the conventional $5 \times 10^5\ M_\odot$; see Bhat *et al.* 1985), a significant fraction of the Oort cloud should in fact remain intact up to the present.

6. External galaxies

6.1. *Introduction*

In previous sections we have presented evidence from various wavebands that indicate that α_{20} may not be constant in the Galaxy but decreases as R decreases. The decrease in α_{20} is roughly consistent with a metallicity dependence: $\alpha_{20} \approx M^{-1}$, although, as pointed out in §4.1, other effects could be simulating this dependence. In view of the widespread application of local calibrations of α_{20} to external galaxies (e.g. Young & Scoville 1982*a*), we examine now an alternative viewpoint: that $\alpha_{20} = \alpha_{20}^{\mathrm{L}}(M_{\mathrm{L}}/M)$ where α_{20}^{L} and M_{L} are the local values of α_{20} and metallicity respectively.

It has been argued on the basis of the apparent lack of correlation between CO luminosity and metallicity for spiral galaxies that the metallicity has at most a weak effect on the CO luminosity (Young *et al.* 1985; Tacconi & Young 1985) and that therefore a constant α_{20} from galaxy to galaxy is justified. However, a plot of L_{CO} against metallicity (e.g. figure 5 of Tacconi & Young 1985) will only reveal a correlation, or lack of it, between CO luminosity and metallicity if the amount of H_2 within the sampled regions is constant.

PHILOSOPHICAL TRANSACTIONS OF THE ROYAL SOCIETY A MATHEMATICAL, PHYSICAL & ENGINEERING SCIENCES

Table 7 gives the mass of H_2 for a sample of galaxies for which both CO and metal abundances have been determined as a function of galactic radius. The metal abundances were derived by fitting a linear relation to log (O/H) + 12 against R, ignoring points very close to the nucleus, for which the excitation and hence abundance are less certain (Pagel & Edmunds 1981). In view of the large scatter in metal abundances that is observed at any particular galactocentric radius, this technique should yield more representative mean abundances, but it should be

TABLE 7. COMPARISON OF H I AND H_2 MASSES BOTH WITH AND WITHOUT METALLICITY CORRECTIONS FOR THOSE GALAXIES WHERE BOTH CO AND METALLICITY HAVE BEEN MEASURED AS A FUNCTION OF GALACTIC RADIUS

(The metallicity-corrected H_2 masses are calculated on the assumption that $M(H_2) \propto L_{CO}/M$ with $\alpha_{20} = 3.0$ at log (O/H) + 12 = 8.9.)

galaxy	distance / Mpc	M(H I) / $10^9 M_\odot$	$M(H_2)$ / $10^9 M_\odot$	$M(H_2)$ ($\alpha_{20} = 8$)	limiting radius / kpc	log (O/H) + 12 at $R = 0$	gradient / dex kpc^{-1}	references
N4321	20	4.6	4.0	29.3	15	9.51	0.02	1, 2, 3
N5194	9.6	2.7	1.7	10.8	10.8	9.65	0.06	1, 4, 5
N5236	8.9	1.5	1.7	11.8	7.8	9.5	0.04	6, 7, 8
N5457	7.2	1.4	3.2	3.4	12	9.1	0.04	9, 10, 11
N6946	10.1	3.2	2.7	11.3	11	9.42	0.06	1, 2, 12
I342	4.5	1.0	0.9	4.3	8	9.43	0.06	1, 2, 13

References: 1, McCall (1982); 2, Young & Scoville (1982*a*); 3, Helou *et al.* (1981); 4, Scoville & Young (1983); 5, Weliachew & Gottesman (1973); 6, Combes *et al.* (1978); 7, Dufour *et al.* (1980); 8, Rogstad *et al.* (1974); 9, Diaz & Tosi (1984); 10, Solomon *et al.* (1983); 11, Bosma *et al.* (1981); 12, Rogstad & Shostak (1972); 13, Newton (1980).

noted that in most cases there are rather few abundance measurements available and the fits are correspondingly uncertain. Table 7 shows that after 'metallicity-correction' of the CO luminosities, the masses of H I and H_2 within the sampled area are comparable, whereas without applying the metallicity correction, H_2 is dominant. Since $\sigma(H_2)$ is now more comparable with σ(H I), the molecular gas tends to 'fill in' the central holes in the H I distribution to give much flatter total gas distributions $\sigma(H\,I + H_2)$. This is in marked contrast to the situation with α_{20} = constant (see, for example, Young & Scoville 1982*a*), although a large part of the difference arises through the adoption of $\alpha_{20}^{L} = 3.0$ rather than 8.

6.2. *Correlation of L_B with L_{CO}*

In view of the good correlations that have been found between L_{CO} and L_B, the blue luminosity (Young & Scoville 1982*b*) we discuss now the implications of our metallicity corrections. On the assumption that $L_{CO} \propto M(H_2)$ and that L_B is a measure of the current rate of star formation, the correlation between L_{CO} and L_B has been interpreted as implying that the rate of star formation per nucleon is constant in both the nuclei and discs of the galaxies studied. On our interpretation, it is L_{CO}/M that is proportional to $M(H_2)$. Figure 13 shows the correlation of L_{CO}/M against L_B for the discs and nuclei of the galaxies listed in Young & Scoville (1982*b*). NGC 1068 is omitted since no metallicity data were available for this galaxy. The results are presented in table 8. In both cases, the scatter about the fitted line was greater for the metallicity-corrected data, but the fit is better from the point of view that L_B is now more nearly directly proportional to $M(H_2)$. Young & Scoville (1982*b*) obtained

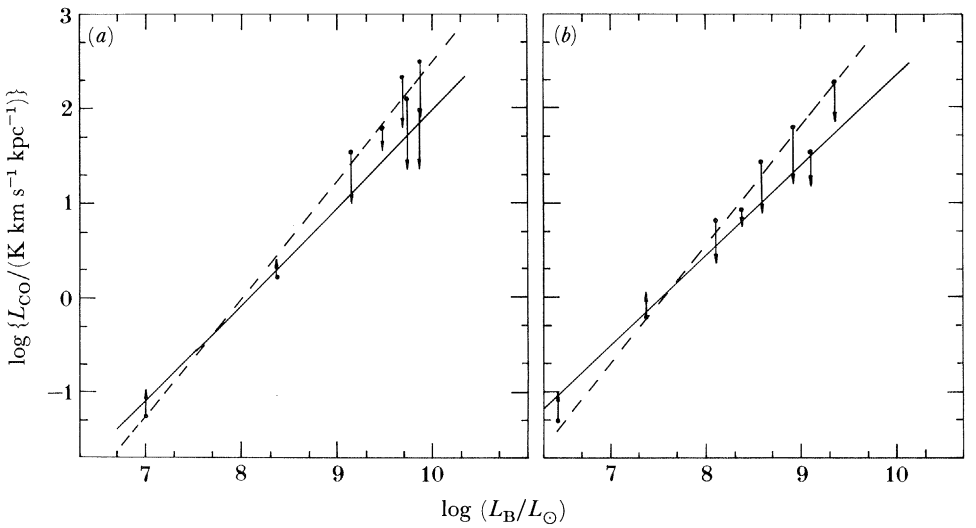

FIGURE 13. L_{CO} plotted against L_B for the nuclei and discs of the galaxies in the work of Young & Scoville (1982): (*a*) central 50″; (*b*) 50″ in discs. The arrows indicate the size of the metallicity correction applied. The broken lines are the best fits as determined by Young & Scoville. The solid lines are the fits after the metallicity corrections have been applied.

TABLE 8. CORRELATIONS BETWEEN L_B AND L_{CO} FOR THE DATA SHOWN IN FIGURES 13 AND 14

(The relations fitted were of the form $L_B = AL_{CO}^a$. The values with no metallicity correction are from Young & Scoville (1982*b*). The appropriate units for L_B and L_{CO} are $L_\odot$ and K km s^{-1} kpc^2 respectively.)

	nuclei		discs	
	A	a	A	a
metallicity-corrected	1.1×10^8	0.98	3.4×10^7	1.06
no correction	1.0×10^8	0.80	3.5×10^7	0.80

$L_B = 4 \times 10^7\ L_{CO}^{1.0}$ for the central 2.5 kpc of their sample of galaxies. No significant correlation could be found after correcting L_{CO} for metallicity, because no metallicity was available for NGC 1068 whereas NGC 2403 and M33 only have upper limits to L_{CO} leaving a very restricted range of L_B and L_{CO}.

Although the correlation obtained for this sample of galaxies is quite good, the correlation between L_B and L_{CO} within a particular galaxy is not so satisfactory. As pointed out by Young & Scoville (1982*b*), for a given CO luminosity, the B luminosity in the nucleus is approximately three times that of a point in the disc, so within a galaxy CO luminosity cannot follow L_B. The most likely explanation is that there is a bulge contribution to L_B in the nucleus that is not directly related to the current rate of star formation. Evidence in favour of this explanation has been given by Young *et al.* (1985), who find a difference in the $L_{CO}-L_B$ correlation for early and late type spirals in the sense expected owing to the more prominent bulge of the early type galaxies.

Detailed surface photometry is available for most of the galaxies in Young & Scoville's sample and so an estimate can be made of the bulge contribution. The results, both with and without metallicity corrections, are given in figure 14. In both cases, the data are scattered about the

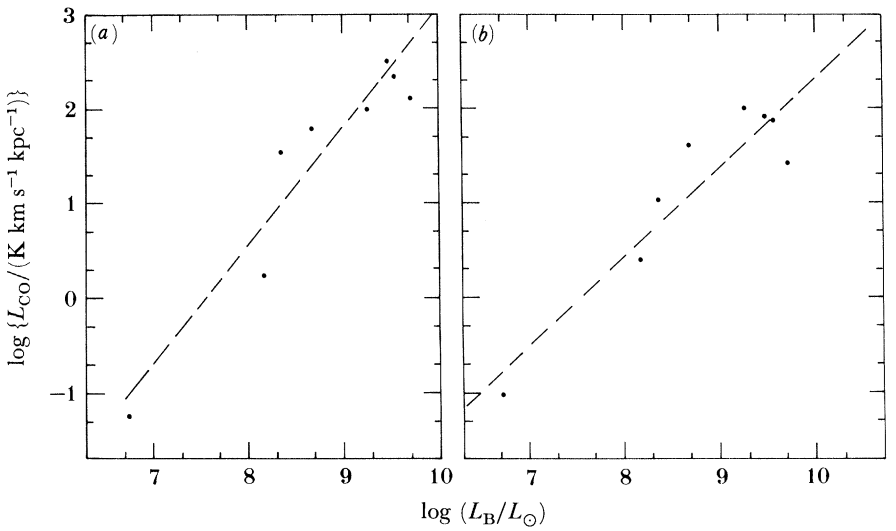

FIGURE 14. L_{CO} plotted against L_B for the nuclei (central 50″) of the galaxies plotted in figure 13. In both cases a bulge component has been subtracted from the quoted blue luminosities. (*a*) The broken line is Young & Scoville's (1982) fit to their disc data; (*b*) a metallicity correction has been applied. The broken line is the best fit to the metallicity-corrected disc data in figure 13.

correlation obtained for the discs but the scatter is large. In view of the uncertainties in these plots for the nuclear regions, i.e. the necessity of extrapolating both the disc light and metallicity into the central regions, it may be preferable to restrict attention to the discs. For those galaxies where detailed photometry, radial profiles of CO emission and metallicity gradient data are available, there is evidence both for and against metallicity corrections if one assumes that L_B should be proportional to $M(H_2)$, i.e. that the quantity of molecular gas alone determines the rate of star formation. Thus L_B follows L_{CO} in the cases of M101 and NGC 6946, whereas L_{CO}/M appears a better fit for IC342 and M83. For M51 neither L_{CO} nor L_{CO}/M follows the steep increase in L_B owing to the inner disc, but L_{CO}/M is a better fit to the outer disc.

Although there is evidence both for and against metallicity's being the cause of the variations in α_{20} from galaxy to galaxy, the evidence that there are variations (which may be partly due to metallicity but also may be excitation, etc.) is unequivocal. This is most clearly seen in the recent work of Rickard & Blitz (1985), who have shown that the ratio $\int T(^{12}CO)\,dv/\int T(^{13}CO)\,dv$ is not constant within a galaxy. Since α_{20} contains the ratio of these two quantities, clearly it must change. One could still argue for a universal conversion factor between $N(H_2)$ and $\int T(^{13}CO)\,dv$, although Rickard & Blitz (1985) have cautioned against this because there may well be opposing variations, e.g. metallicity and temperature, which act in opposite ways on the $\int T(^{12}CO)\,dv/\int T(^{13}CO)\,dv$ ratio.

A further argument in favour of a variable α_{20} comes from abundance measurements in the Small Magellanic Cloud (SMC). Dufour (1984) has recommended a total carbon abundance relative to hydrogen of only 1.4×10^{-5}, i.e. a value one twenty-sixth that of the solar abundance. S.S.S. have argued that their value of α_{20} (= 7.2) is equivalent to the adoption of LTE with $^{13}CO/H_2 = 10^{-6}$; thus, for a ratio $^{12}C/^{13}C = 60$ and $C/H_\odot = 3.72\times10^{-4}$, then locally *ca.* 8% of the available carbon is locked up in CO. The minimum α_{20} in the SMC then follows as *ca.* 15, assuming that all the carbon is in CO. This may be possible in view of the absence

of the 2200 Å† feature in the reddening curve of the SMC (Nandy 1984), this feature being widely interpreted as indicating the presence of graphite grains.

Although the above argument shows that α_{20} must be different from the galactic value it also illustrates a further uncertainty in the metallicity corrections proposed earlier. Both in the SMC and the Large Magellanic Cloud (LMC) the oxygen abundance is less depleted than the carbon abundance. Specifically, oxygen is less by factors of 3 and 8 for the LMC and SMC respectively, whereas carbon is depleted by factors of 5 and 26 (Dufour 1984). Clearly in these two galaxies the oxygen and carbon abundances do not go hand in hand. This may also be the case for those galaxies in table 7 with oxygen abundances greater than solar. If the carbon abundances there were not as enhanced as those of oxygen the proposed metallicity corrections could be too large.

Israel (1984) has pointed out that the CO intensities in the Magellanic clouds are lower than expected from an extrapolation of Galactic GMCs to Magellanic distances by a factor 2–4 in the LMC (and the SMC–SW bar) and by at least a factor six in the rest of the SMC. However, the mean dark cloud masses determined from extinction are $1\text{–}1.5 \times 10^5\ M_\odot$ when the appropriate gas:dust ratios are applied, very similar to our estimate of galactic GMC mass. The implication is that α_{20} is larger in the LMC and SMC than locally by factors roughly proportional to the mean metallicity decrease (Bhat *et al.* 1984).

An alternative approach to the question of the gas content of galactic nuclei has been followed by Rickard & Harvey (1984). They use far infrared radiation to measure the dust mass. After assuming the canonical dust:gas ratio of 0.01, they derive $\sigma(\mathrm{H_2})/\int T(^{12}\mathrm{CO})\,\mathrm{d}v = 1.0\ M_\odot\ \mathrm{pc^{-2}\ K^{-1}\ km^{-1}\ s}$, which corresponds to $\alpha_{20} = 2.5$. Noting that this value is somewhat low compared with values often quoted, they issue the caveat that their α_{20} may be a lower limit owing to underestimating contributions from cold dust or may indicate the presence of unusual gas:dust ratios. The two galaxies in their list for which they quote mass surface densities of dust and for which we have estimated metallicity corrections, i.e. NGC 6946 and IC342, both have $\sigma_{\mathrm{gas}} = 22\ M_\odot\ \mathrm{pc^{-2}}$ on the basis of their IR emission. Our estimates for these galaxies are $\sigma(\mathrm{H_2{+}HI}) = 33$ and $22\ M_\odot\ \mathrm{pc^{-2}}$ respectively, whereas Young & Scoville (1982*a*) derive 260 and $220\ M_\odot\ \mathrm{pc^{-2}}$. The only other galaxy for which we could find metal abundances, CO measurements and a measured rather than inferred dust temperature was M51. For $T_{\mathrm{d}} = 20$ K (Smith 1982), $\sigma_{\mathrm{gas}} \approx 170\ M_\odot\ \mathrm{pc^{-2}}$ for a dust:gas ratio of 0.01. This is in good agreement with Young & Scoville (1982*a*) who infer $\sigma_{\mathrm{H_2}} \approx 190\ M_\odot\ \mathrm{pc^{-2}}$ but not with our metallicity-corrected value $\sigma(\mathrm{HI{+}H_2}) \approx 15\ M_\odot\ \mathrm{pc^{-2}}$. The uncertainties in these estimates are large owing to the sensitivity of the dust mass to the inferred temperature and the likelihood of the dust:gas ratio also being a function of the metallicity. Until larger samples become available no firm conclusions can be derived but at present the far IR emission indicates a considerable spread in σ_{20} (Rickard & Harvey 1984) from $\alpha_{20} = 0.5$ (NGC 2903) to $\alpha_{20} = 20.5$ (NGC 4303).

7. Conclusions

A variety of techniques have been employed to derive the local value of α_{20}, the conversion factor between CO line intensity and $\mathrm{H_2}$ column density; all were shown to be consistent with α_{20} in the range 2–4. There is strong evidence that α_{20} is much smaller at the Galactic Centre

† $1\ \text{Å} = 10^{-10}\ \mathrm{m} = 10^{-1}\ \mathrm{nm}$.

(specifically $\alpha_{20} \approx 0.5$) with some evidence that α_{20} falls steadily from its local value to $\alpha_{20} \lesssim 1.8$ at the Molecular Ring. This has major implications for the mass of molecular hydrogen in the Galaxy, and a value of $6.1 \times 10^8\ M_\odot$ was derived for $R \leqslant 10$ kpc (but excluding the Galactic Centre). If α_{20} is constant outside the Galactic Centre then $M(\mathrm{H_2}) = 9.8 \times 10^8\ M_\odot$.

In paper I we argued that a decrease in α_{20} in the inner Galaxy was probably due to a metallicity effect. More recent work on external galaxies points strongly towards large-scale variations in α_{20}, but factors other than metallicity appear to be causing most of these variations. Thus whether metallicity as such is important or not in our Galaxy, both theoretically and observationally there is no *a priori* reason why α_{20} should remain constant as a function of Galactocentric radius. We are still of the opinion, therefore, that a systematic (and also, no doubt, a point-to-point) variation of α_{20} with R occurs.

It is important that the techniques of §3 be extended to larger samples of objects, particularly the X-ray method as this alone samples the metals in both the gas and grain phases. In particular, measurements in the anticentre direction would enable an estimate to be made of α_{20} at $R > 10$ kpc, which would extend the baseline over which to look for variations in α_{20} and would enable a better estimate to be made of the amount of gas in the outer Galaxy. Present estimates indicate a sharp fall in the surface density of $\mathrm{H_2}$ for $R > 10$ kpc whereas the distribution of 'young' objects, e.g. pulsars, HII regions and SNR, and the star formation rate (Bhat *et al.* 1984; Rana & Wilkinson 1985) show a much smoother decline. The implication is that either the efficiency of processing gas in the outer Galaxy is high or, more likely, there is more molecular hydrogen than currently believed.

The authors are grateful to Professor D. A. Williams for many helpful discussions relating to interstellar chemistry. Dr T. M. Dame, Dr D. B. Sanders and Dr Judith Young are thanked for useful comments, and the referee is thanked for constructive criticisms. We are grateful to our co-workers who have contributed to this subject in many ways: Professor M. R. Issa and Dr B. P. Houston. The Science and Engineering Research Council is thanked for its support.

References

Adams, D. J. 1980 In *Cosmic X-ray astronomy* (*Monographs on astronomical subjects*) (ed. A. J. Meadows), p. 58. Bristol: Adam Hilger.
Aitken, D. K. & Jones, B. 1973 *Astrophys. J.* **184**, 127.
Bailey, M. E. 1983 *Mon. Not. R. astr. Soc.* **204**, 603.
Basinka, E. M., Lewin, W. H. G., Szatjno, M., Cominsky, L. R. & Marshall, F. J. 1984 *Astrophys. J.* **281**, 337.
Becker, R. H., Boldt, E. A., Holt, S. S., Serlemitsos, P. J. & White, N. E. 1980 *Astrophys. J. Lett.* **237**, L77.
Becker, R. H. & Helfand, D. J. 1984 *Astrophys. J.* **283**, 154.
Becker, R. H., Helfand, D. J. & Szymkowiak, A. E. 1982 *Astrophys. J.* **255**, 612.
Becker, R. H. & Szymkowiak, A. E. 1981 *Astrophys. J. Lett.* **248**, L23.
Becklin, E. E., Matthews, K., Neugebauer, G. & Willner, S. P. 1978 *Astrophys. J.* **220**, 831.
Becklin, E. E. & Neugebauer, G. 1968 *Astrophys. J.* **151**, 145.
Bedford, D. K., Carpenter, G. F., Goodall, C. V., Pollock, A. M. T., Cole, R. E., Cruise, A. M. & Osborne, J. P. 1981 *Space Sci. Rev.* **30**, 373.
Bell-Burnell, S. J. & Chiappetti, L. 1984 *Astron. Astrophys. Suppl.* **56**, 415.
Bhat, C. L., Houston, B. P., Issa, M. R., Mayer, C. J. & Wolfendale, A. W. 1984 *Proc. Abingdon I.S.M. Conf.*, p. 39.
Bhat, C. L., Issa, M., Houston, B. P., Mayer, C. J. & Wolfendale, A. W. 1985 *Nature, Lond.* **314**, 511.
Blecker, J., Deerenberg, A., Yamashita, K., Hayakawa, S. & Tanaka, Y. 1972 *Astrophys. J.* **178**, 377.
Blitz, L. 1978 Ph.D. thesis, Columbia University.
Blitz, L., Bloemen, J. D. G. M., Hermsen, W. & Bania, T. M. 1985 *Astron. Astrophys.* **143**, 267.
Blitz, L. & Shu, F. H. 1980 *Astrophys. J.* **238**, 148.

PHILOSOPHICAL TRANSACTIONS OF THE ROYAL SOCIETY A MATHEMATICAL, PHYSICAL & ENGINEERING SCIENCES

Bloemen, J. B. G. M., Bennett, K., Bignami, G. F., Blitz, L., Caraveo, P. A., Gottwald, M., Hermsen, W., Lebrun, F., Mayer-Hasselwander, H. A. & Strong, A. W. 1984 *Astron. Astrophys.* **139**, 37.
Bohlin, R. C., Savage, B. D. & Drake, J. F. 1978 *Astrophys. J.* **224**, 132.
Bosma, A., Goss, W. M. & Allen, R. J. 1981 *Astron. Astrophys.* **93**, 106.
Brandt, H. V. D. & McClintock, J. E. 1983 *A. Rev. Astr. Astrophys.* **21**, 13.
Brown, R. L. & Gould, R. 1970 *Phys. Rev.* D **1**, 2252.
Brown, R. L. & Liszt, H. S. 1984 *A. Rev. Astr. Astrophys.* **22**, 223.
Branduardi, H., Ives, J. C., Sanford, P. W., Brinkman, A. C. & Marashi, L. 1976 *Mon. Not. R. astr. Soc.* **175**, *P*47.
Bregman, J., Butler, D., Kemper, E., Koski, A., Kraft, R. P. & Stone, R. P. J. 1973 *Astrophys. J. Lett.* **185**, L117.
Burginyon, C., Hill, R., Palmieri, T., Scudder, J., Stoering, J. & Toor, A. 1973 *Astrophys. J.* **179**, 615.
Burginyon, G. A., Hill, R. W. & Seward, F. D. 1975 *Astrophys. J.* **200**, 163.
Burton, W. B. 1976 *The structure and content of the Galaxy and Galactic gamma rays.* Greenbelt, Maryland: Goddard Space Flight Centre.
Burton, W. B. & Gordon, M. A. 1978 *Astron. Astrophys.* **63**, 7.
Caswell, J. L., Murray, J. D., Roger, R. S. & Cole, D. J. 1975 *Astron. Astrophys.* **45**, 239.
Charles, P. A., Culhane, J. L. & Tuohy, I. R. 1973 *Mon. Not. R. astr. Soc.* **165**, 355.
Charles, P. A., Culhane, J. L., Zarnecki, J. C. & Fabian, A. C. 1975 *Astrophys. J. Lett.* **197**, L61.
Charles, P. A., Kahn, S. M., Bowyer, S., Blissett, R. J., Culhane, J. L., Cruise, A. M. & Garmire, G. 1979 *Astrophys. J. Lett.* **230**, L83.
Chiappetti, L. & Bell-Burnell, S. J. 1981 *Space Sci. Rev.* **30**, 389.
Clark, G. W., Bradt, H. V., Lewin, W. H. G., Markard, T. H., Schnopper, H. W. & Sprott, G. F. 1973 *Astrophys. J.* **179**, 263.
Clube, S. V. M. & Napier, W. M. 1982 *Q. Jl R. astr. Soc.* **23**, 45.
Cohen, R. S. & Thaddeus, P. 1977 *Astrophys. J. Lett.* **217**, L155.
Combes, F., Encrenaz, P. J., Lucas, R. & Weliachew, L. 1978 *Astron. Astrophys.* **67**, L13.
Cornett, R. H., Chin, G. & Knapp, G. R. 1977 *Astron. Astrophys.* **54**, 889.
Cruddace, R., Bowyer, S., Lampton, M., Mack, J. & Margon, B. 1972 *Astrophys. J.* **177**, 529.
Cruddace, R., Fritz, G., Shubman, S., Friedman, H., McKnee, J. & Johnson, M. 1978 *Astrophys. J. Lett.* **222**, L95.
Cruddace, R., Paresec, F., Bowyer, S. & Lampton, M. 1974 *Astrophys. J.* **187**, 497.
Culhane, J. L. 1977 In *Supernovae* (ed. D. N. Schramm), p. 29. Dordrecht: D. Reidel.
Dame, T. 1984 Ph.D. thesis, Columbia University.
Davelaar, J., Bleeker, J. A. M., Deeremberg, A. J. M., Tanaka, Y., Hayakawa, S. & Yamashita, K. 1978 In *COSPAR/IAU Symp. on X-ray Astronomy, Innsbruck*, p. 54.
Diaz, A. I. & Tosi, M. 1984 *Mon. Not. R. astr. Soc.* **208**, 365.
Dickel, J. R. 1973 *Astrophys. Lett.* **15**, 61.
Dickman, R. L. 1978 *Astrophys. J. Suppl.* **37**, 407.
Dufour, R. J. 1984 In *Structure and evolution of the Magellanic Clouds* (*I.A.U. Symp.* no. 108) (ed. S. van den Bergh & K. S. de Boer), p. 353. Dordrecht: D. Reidel.
Dufour, R. J., Talbot, R. J., Jensen, E. P. & Shields, G. A. 1980 *Astrophys. J.* **236**, 119.
Eaton, N., Adams, D. J. & Giles, A. B. 1984 *Mon. Not. R. astr. Soc.* **208**, 241.
Ecran, E. N. & Cruise, A. M. 1984 *Mon. Not. R. astr. Soc.* **209**, 271.
Fabian, A. C., Willingale, R., Pye, J. P., Murray, S. S. & Fabbiano, G. 1980 *Mon. Not. R. astr. Soc.* **193**, 175.
Fireman, E. L. 1974 *Astrophys. J.* **187**, 57.
Frerking, M. A., Langer, W. D. & Wilson, R. W. 1982 *Astrophys. J.* **262**, 590.
Fritz, G., Meekins, J. F., Chubb, T. A., Friedman, H. & Henry, R. C. 1971 *Astrophys. J. Lett.* **164**, L55.
Garmire, G. & Fiegler, G. R. 1972 *Astron. Astrophys.* **21**, 131.
Gatley, I. 1982 In *The Galactic Centre* (ed. G. R. Reigler & R. D. Blandford), p. 25. New York: American Institute of Physics.
Gorenstein, P. 1975 *Astrophys. J.* **198**, 95.
Gorenstein, P., Kellog, E. M. & Gursky, H. 1970 *Astrophys. J.* **160**, 199.
Gorenstein, P., Haruden, F. R. Jr & Tucker, W. H. 1974 *Astrophys. J.* **192**, 661.
Grader, R. J., Hill, R. W. & Stoering, J. P. 1970 *Astrophys. J. Lett.* **161**, L45.
Greenberg, J. M. & Hong, S. S. 1974 In *HII regions and the Galactic Centre* (*8th ESLAB Symp., Italy*), ESRO SP-105, p. 221.
Grindlay, J. E. 1981 In *X-ray astronomy with Einstein Observatory* (ed. R. Giacconi), p. 79. Dordrecht: D. Reidel.
Grindlay, J. E. & Hertz, P. 1981 *Astrophys. J. Lett.* **277**, L17.
Helou, G., Giovanardi, C., Salpeter, E. E. & Krumm, G. 1981 *Astrophys. J. Suppl.* **46**, 267.
Henry, R. C., Fritz, G., Meekins, J. F., Chubb, T. A. & Friedman, H. 1972 *Astrophys. J.* **174**, 389.
Hermsen, W. 1980 Ph.D. thesis, University of Leiden.
Hermsen, W. & Bloemen, J. B. G. M. 1983 In *Surveys of the southern Galaxy* (ed. W. B. Burton & F. P. Israel), p. 65. Dordrecht: D. Reidel.

PHILOSOPHICAL TRANSACTIONS OF THE ROYAL SOCIETY A MATHEMATICAL, PHYSICAL & ENGINEERING SCIENCES

Hertz, P. & Grindlay, J. E. 1984 *Astrophys. J.* **282**, 118.
Hill, R. W., Burginyon, G. A. & Seward, F. D. 1975 *Astrophys. J.* **200**, 158.
Hoffman, J. A., Lewin, W. H. G., Primini, F. A., Wheaton, W. A., Swank, J. H., Boldt, E. A., Holt, S. S., Serlemitsos, P. J., Share, G. H., Wood, K., Yentis, D., Evans, W. D., Matteson, J. L., Grubber, D. E. & Peterson, L. E. 1979 *Astrophys. J. Lett.* **233**, L51.
Holt, S. S. 1983 In *Supernova remnants and their X-ray emissions* (ed. J. Danziger & P. Gorenstein), p. 17. Dordrecht: D. Reidel.
Houston, B. P. & Wolfendale, A. W. 1984 *J. Phys.* G **10**, 1587.
Houston, B. P. & Wolfendale, A. W. 1985 *J. Phys.* G **11**, 407.
Israel, F. P. 1984 In *Structure and evolution of the Magellanic Clouds* (*I.A.U. Symp.* no. 108) (ed. S. van den Bergh & K. S. de Boer), p. 319. Dordrecht: D. Reidel.
Issa, M. R. & Wolfendale, A. W. 1981 *Nature, Lond.* **292**, 430.
Jones, C. 1977 *Astrophys. J.* **214**, 856.
Jones, C., Forman, W., Tanenbaum, H., Schreier, E., Gursky, H., Kellog, E. & Giacconi, R. 1973 *Astrophys. J. Lett.* **181**, L43.
Kahn, S. M., Charles, P. A., Bowyer, S. & Blissett, R. J. 1980 *Astrophys. J. Lett.* **242**, L19.
Kahn, S. M., Brodie, J., Bowyer, S. & Charles, P. A. 1983 *Astrophys. J.* **269**, 212.
Kahn, S. M., Seward, F. D. & Chlebowski, T. 1984 *Astrophys. J.* **283**, 286.
Kayat, M. A., Rolf, D. P., Smith, G. C. & Willingale, R. 1980 *Mon. Not. R. astr. Soc.* **191**, 729.
Kiang, T. 1968 *Reduced counts of galaxies along Galactic coordinates* (*Dunsink Observatory Pubs*, vol. 1, no. 5). Dublin.
Ku, W. H. M., Long, K., Pisarski, R. & Vartanian, M. 1983 In *Supernova remnants and their X-ray emission* (ed. J. Danziger & P. Gorenstein), p. 253. Dordrecht: D. Reidel.
Kutner, M. L. & Leung, C. M. 1985 *Astrophys. J.* **291**, 188.
Kutner, M. L. & Mead, K. N. 1981 *Astrophys. J. Lett.* **249**, L15.
Lada, C. J. 1976 *Astrophys. J. Suppl.* **32**, 603.
Lamb, P. & Sanford, P. W. 1979 *Mon. Not. R. astr. Soc.* **188**, 555.
Larson, R. B. 1981 *Mon. Not. R. astr. Soc.* **194**, 809.
Lebrun, F., Bennett, K., Bignami, G. F., Bloemen, J. B. G. M., Buccheri, R., Caraveo, P. A., Gottwald, M., Hermsen, W., Kanbach, G., Mayer-Hasselwander, H. A., Montmerle, T., Paul, J. A., Sacco, B., Strong, A. W., Wills, R. D., Dame, T. M., Cohen, R. S. & Thaddeus, P. 1983 *Astrophys. J.* **274**, 231.
Lebrun, F. & Huang, Y.-L. 1984 *Astrophys. J.* **281**, 634.
Leibowitz, E. M. & Danziger, I. J. 1983 *Mon. Not. R. astr. Soc.* **204**, 273.
Leung, C. M. & Liszt, H. S. 1976 *Astrophys. J.* **208**, 732.
Lewin, W. H. G., Hoffman, J. A., Doty, J., Hearn, D. R., Clark, G. W., Jeringan, J. G., Li, F. K., McClintock, J. E. & Richardson, J. 1976 *Mon. Not. R. astr. Soc.* **177**, 83.
Li, Ti pei, Riley, P. A. & Wolfendale, A. W. 1983 *Mon. Not. R. astr. Soc.* **302**, 87.
Li, Ti pei & Wolfendale, A. W. 1981 *Astron. Astrophys.* **103**, 19.
Lieu, R., Verkatesan, D. & Kitani, K. 1984 *Astrophys. J.* **282**, 709.
Linke, R. A., Stark, A. A. & Frerking, M. A. 1981 *Astrophys. J.* **243**, 147.
Liszt, H. S. & Burton, W. B. 1980 *Astrophys. J.* **236**, 779.
Liszt, H. S. & Burton, W. B. 1981 *Astrophys. J.* **243**, 778.
Liszt, H. S., Burton, W. B. & Xiang, D.-L. 1984 *Astron. Astrophys.* **140**, 303.
Liszt, H. S., Xiang, D.-L. & Burton, W. B. 1981 *Astrophys. J.* **249**, 532.
Longmore, A. J., Clark, D. H. & Murdin, P. 1977 *Mon. Not. R. astr. Soc.* **181**, 571.
Loren, R. B., Peters, W. L. & van den Bout, P. A. 1974 *Astrophys. J. Lett.* **194**, L103.
McCall, M. L. 1982 Ph.D. thesis, University of Texas at Austin.
Margon, B., Bowyer, S. & Stone, R. P. S. 1973 *Astrophys. J. Lett.* **185**, L113.
Markert, T. H., Lamb, R. C., Hartman, R. C., Thompson, D. J. & Bignami, G. F. 1981 *Astrophys. J. Lett.* **248**, L17.
Markert, T. H., Winkler, P. F., Laird, F. N., Clark, G. W., Hearn, D. R., Sprott, G. F., Li, F. K., Bradt, H. V., Lewin, W. H. G. & Schropper, H. W. 1979 *Astrophys. J. Suppl.* **39**, 573.
Martin, H. M., Sanders, D. B. & Hill, R. E. 1984 *Mon. Not. R. astr. Soc.* **208**, 35.
Matsumoto, T., Hayakawa, S., Koizumi, H., Murakani, H., Ugama, K., Yamagami, T. & Thomas, J. A. 1982 In *The Galactic Centre* (ed. G. R. Riegler & R. D. Blandford), p. 48. New York: American Institute of Physics.
Matteson, J. L. 1982 In *The Galactic Centre* (ed. G. R. Riegler & R. D. Blandford), p. 109. New York: American Institute of Physics.
Mihalas, D. & Binney, J. 1981 In *Galactic astronomy – structure and kinematics*, p. 180. San Francisco: W. H. Freeman.
Miller, J. S. 1973 *Astrophys. J. Lett.* **180**, L83.
Moore, W. E., Cordova, F. & Garmire, G. P. 1973 In *13th Int. Cosmic Ray Conf.*, vol. 1, p. 56.
Moore, W. E. & Garmire, G. P. 1976 *Astrophys. J.* **206**, 247.
Morrison, R. & McCannon, D. 1983 *Astrophys. J.* **207**, 119.
Murry, S. S., Fabbiano, G., Fabian, A. C., Epstein, A. & Giacconi, R. 1979 *Astrophys. J. Lett.* **234**, L69.

PHILOSOPHICAL TRANSACTIONS OF THE ROYAL SOCIETY A MATHEMATICAL, PHYSICAL & ENGINEERING SCIENCES

Myers, P. C. 1983 *Astrophys. J.* **270**, 105.
Nandy, K. 1984 In *Structure and evolution of the Magellanic Clouds* (*I.A.U. Symp.* no. 108) (ed. S. van den Bergh & K. S. de Boer), p. 341. Dordrecht: D. Reidel.
Napier, W. M. & Staniuchi, M. 1982 *Mon. Not. R. astr. Soc.* **198**, 723.
Newton, K. 1980 *Mon. Not. R. astr. Soc.* **191**, 615.
Nugent, J. J., Pravdo, S. H., Gordon, P. G., Becker, R. H., Tuohy, I. R. & Winkler, P. F. 1984 *Astrophys. J.* **284**, 612.
Okuda, H., Mahara, T., Oda, N. & Sugiyani, T. 1979 In *The large scale characteristics of the Galaxy* (*I.A.U. Symp.* no. 84) (ed. W. B. Burton), p. 377. Dordrecht: D. Reidel.
Oort, J. H. 1977 *A. Rev. Astr. Astrophys.* **15**, 295.
Page, C. G. 1981 *Space Sci. Rev.* **30**, 369.
Pagel, B. E. J. & Edmunds, M. G. 1981 *A. Rev. Astr. Astrophys.* **19**, 77.
Palmieri, T. M., Burginyon, G., Grader, R. J., Hill, R. W., Seward, F. D. & Stoering, J. P. 1971 *Astrophys. J.* **164**, 61.
Parker, R. A. R. 1967 *Astrophys. J.* **149**, 363.
Parsignault, D. R. & Grindlay, J. E. 1978 *Astrophys. J.* **225**, 970.
Peimbert, M. 1982 *Annls New York Acad. Sci.* **395**, 24.
Petre, R., Canizares, C. R., Winkler, P. F., Seward, F. D., Willingale, R., Rolf, D. & Woods, N. 1983 In *Supernova remnants and their X-ray emission* (*I.A.U. Symp.* no. 101) (ed. J. Danziger & P. Gorenstein), p. 289. Dordrecht: D. Reidel.
Pollock, A. M. T., Goodall, C. V., Carpenter, C. F., Bedford, D. K., Gruise, A. M., Cole, R. E., Osborne, J. P. & Culhane, J. L. 1981 *Space Sci. Rev.* **30**, 347.
Pravdo, S. H., Becker, R. H., Boldt, E. A., Holt, S. S., Rochschild, R. E., Serlemisos, P. J. & Swank, J. H. 1976 *Astrophys. J. Lett.* **206**, L41.
Pravdo, S. H., Smith, B. E., Charles, P. A. & Tuohy, I. R. 1980 *Astrophys. J. Lett.* **235**, L9.
Proctor, R. J., Skinner, G. K. & Willmore, A. P. 1978 *Mon. Not. R. astr. Soc.* **185**, 745.
Pye, J. P., Becker, R. H., Seward, F. D. & Thomas, N. 1984 *Mon. Not. R. astr. Soc.* **207**, 649.
Radhakrishnan, V., Goss, W. M., Murray, J. D. & Brooks, J. W. 1972 *Astrophys. J. Suppl.* **24**, 49.
Rana, N. C. & Wilkinson, D. A. 1986 *Mon. Not. R. astr. Soc.* **218**, 497.
Rappaport, S., Doxsey, R., Solinger, A. & Borken, R. 1974 *Astrophys. J.* **194**, 329.
Raymond, J. C., Black, J. H., Dupree, A. K., Hartmann, L. & Wolff, R. S. 1981 *Astrophys. J.* **246**, 100.
Reid, P. B., Becker, R. H. & Long, K. S. 1981 *Astrophys. J.* **261**, 485.
Reynolds, R. J. & Ogden, P. M. 1978 *Astrophys. J.* **220**, 172.
Rickard, L. J. & Blitz, L. 1985 *Astrophys. J.* **292**, L57.
Rickard, L. J. & Harvey, P. M. 1984 *Astron. J.* **89**, 1520.
Ride, S. K. & Walker, A. B. C. 1977 *Astron. Astrophys.* **61**, 339.
Robinson, B. J., Manchester, R. N., Whiteoak, J. B., Sanders, D. B., Scoville, N. Z., Clemens, D. P. & Solomon, P. M. 1984 *Astrophys. J. Lett.* **283**, L31.
Rogstad, D. H., Lockhart, I. A. & Wright, M. C. H. 1974 *Astrophys. J.* **193**, 309.
Rogstad, D. H. & Shostak, G. S. 1972 *Astrophys. J.* **176**, 315.
Ryter, C., Cesarsky, C. J. & Audouze, J. 1975 *Astrophys. J.* **198**, 103.
Sanders, D. B. 1981 Ph.D. thesis, State University of New York at Stony Brook.
Sanders, D. B., Scoville, N. Z. & Solomon, P. M. 1985 *Astrophys. J.* **289**, 373.
Sanders, D. B., Solomon, P. M. & Scoville, N. Z. 1984 *Astrophys. J.* **276**, 182.
Savage, D. B. & Mathis, J. S. 1979 *A. Rev. Astr. Astrophys.* **17**, 73.
Scoville, N. Z., Irvine, W. M., Wannier, P. G. & Predmore, C. R. 1977 *Astrophys. J.* **216**, 320.
Scoville, N. Z. & Solomon, P. M. 1975 *Astrophys. J. Lett.* **199**, L105.
Scoville, N. Z. & Young, J. S. 1983 *Astrophys. J.* **265**, 148.
Serlemitsos, P. J., Boldt, E. A., Holt, S. S., Ramaty, R. & Brisken, A. F. 1973 *Astrophys. J. Lett.* **184**, L1.
Seward, F. D., Burginyon, G. A., Grader, R. J., Hill, R. W., Palmieri, T. M. & Stoering, J. P. 1971 *Astrophys. J.* **169**, 515.
Seward, F. D., Burginyon, G. A., Grader, R. J., Hill, R. W. & Palmieri, T. M. 1972 *Astrophys. J.* **178**, 131.
Seward, F. D., Gorenstein, P. & Tucker, W. 1983 *Astrophys. J.* **266**, 287.
Smith, A., Jones, L. R., Watson, M. G., Willingale, R., Wood, N. & Seward, F. D. 1985 (Preprint.)
Smith, B. W. 1981 In *X-ray astronomy with Einstein satellite* (ed. R. Giacconi), p. 51. Dordrecht: D. Reidel.
Smith, J. 1982 *Astrophys. J.* **261**, 463.
Solomon, P. M., Barrett, J. M., Sanders, D. B. & de Zafra, R. 1983 *Astrophys. J. Lett.* **266**, L103.
Solomon, P. M., Scoville, N. Z. & Sanders, D. B. 1979 *Astrophys. J. Lett.* **232**, L89.
Spinrad, H., Liebert, J., Smith, H. E., Schweizer, F. & Kuti, L. V. 1971 *Astrophys. J.* **165**, 17.
Stark, A. A. 1979 Ph.D. thesis, University of Princeton.
Stark, A. A. & Blitz, L. 1978 *Astrophys. J. Lett.* **225**, L15.
Stella, L., Kahn, S. M. & Grindlay, J. E. 1984 *Astrophys. J.* **282**, 713.

PHILOSOPHICAL TRANSACTIONS OF THE ROYAL SOCIETY A MATHEMATICAL, PHYSICAL & ENGINEERING SCIENCES

Stevens, J. C. & Garmire, G. P. 1973 *Astrophys. J. Lett.* **180**, L19.
Strong, A. W., Bignami, G. F., Bloemen, J. B. G. M., Buccheri, R., Caraveo, P. A., Hermsen, W., Kanbach, G., Lebrun, F., Mayer-Hasselwander, H. A., Paul, J. A. & Wills, R. D. 1982 *Astron. Astrophys.* **115**, 404.
Strong, A. & Lebrun, F. 1982 *Astron. Astrophys.* **105**, 159.
Tacconi, L. J. & Young, J. S. 1985 *Astrophys. J.* **290**, 602.
Tuohy, I. R. & Garmire, G. P. 1980 *Astrophys. J. Lett.* **239**, L107.
Tuohy, I. R., Nousek, J. A. & Garmire, G. P. 1979*a* *Astrophys. J. Lett.* **234**, L101.
Tuohy, I. R., Nugent, J. J., Garmire, G. P. & Clark, D. H. 1979*b* *Nature, Lond.* **279**, 139.
van den Bergh, S. & Kamper, K. W. 1977 *Astrophys. J.* **218**, 617.
Wang, Z. R. & Seward, F. D. 1984 *Astrophys. J.* **279**, 705.
Watson, M. G., Willingale, R., Grindlay, J. E. & Hertz, P. 1981 *Astrophys. J.* **250**, 172.
Watson, M. G., Willingale, R., Pye, J. P., Rolf, D. P., Wood, N., Thomas, N. & Seward, F. D. 1983 In *Supernova remnants and their X-ray emission* (*I.A.U. Symp.* no. 101) (ed. J. Danziger & P. Gorenstein), p. 273. Dordrecht: D. Reidel.
Weaver, H. & Williams, D. R. W. 1973 *Astron. Astrophys. Suppl.* **8**, 1.
Weliachew, L. & Gottesman, S. T. 1973 *Astron. Astrophys.* **24**, 59.
Westerlund, B. E. 1969 *Astron. J.* **74**, 879.
Whelan, J. A. J., Mayo, S. K., Wickramasinghe, D. T., Murdin, P. G., Peterson, B. A., Hawarden, T. G., Longmore, A. J., Haynes, R. F., Goss, W. M., Simons, L. W., Caswell, L. J., Little, A. G. & McAdam, W. B. 1977 *Mon. Not. R. astr. Soc.* **181**, 259.
Whittet, D. C. B., Longmore, A. J. & McFadzean, A. D. 1985 *Mon. Not. R. astr. Soc.* **216**, 45*P*.
William, H. M. *et al.* 1984 *Astrophys. J.* **278**, 615.
Williams, D. A. 1985 *Q. Jl R. astr. Soc.* **26**, 393.
Winkler, P. F. 1978 *Astrophys. J.* **221**, 220.
Winkler, P. F., Canizares, C. R., Clark, G. W., Markert, T. H. & Petrie, R. 1981 *Astrophys. J.* **245**, 574.
Wolfendale, A. W. 1983 *Q. Jl R. astr. Soc.* **24**, 226.
Woltjer, L. 1972 *A. Rev. Astr. Astrophys.* **10**, 129.
Wu, C., Van Diunen, R. J. & Hammerschlag-Hensberge, G. 1975 In *Symp. on X-ray Binaries* (NASA SP-389), p. 102.
Young, J. S. & Scoville, N. Z. 1982*a* *Astrophys. J.* **258**, 467.
Young, J. S. & Scoville, N. Z. 1982*b* *Astrophys. J. Lett.* **260**, L11.
Young, J. S., Scoville, N. Z. & Brady, E. 1985 *Astrophys. J.* **288**, 487.
Zarnecki, J. C. & Bibbo, G. 1979 *Mon. Not. R. astr. Soc.* **186**, 51.
Zarnecki, J. C, Culhane, J. L., Toor, A., Seward, F. D. & Charles, P. A. 1978 *Astrophys. J. Lett.* **219**, L17.

PHILOSOPHICAL TRANSACTIONS OF THE ROYAL SOCIETY A MATHEMATICAL, PHYSICAL & ENGINEERING SCIENCES